Proportional Resonant Control of Power Electronic Interface for Integrating Renewable Energy Sources

By

Rizwan Arshad

NUST201362034MSMME62113F

Supervised by

Dr. Mohsin Jamil

A Thesis Submitted in Partial

Fulfillment of the Requirements for the Degree of

M.S. in

ROBOTICS AND INTELLIGENT MACHINE ENGINEERING

at

School of Mechanical and Manufacturing Engineering (SMME)

National University of Sciences and Technology (NUST),

Islamabad, Pakistan

2015.

Dedicated to my beloved mother and father who have guided me in the journey of education.

FORM TH-4

MASTER THESIS WORK

We hereby recommend that the dissertation prepared under our supervision by:
Student Name: Rizwan Arshad Registration No: NUST201362034MSMME62113F
Titled: Proportional Resonant Control of Power Electronic Interface for Integrating Renewable Energy Sources be accepted in partial fulfillment of the requirements for the award of MS in Robotics And Intelligent Machine Engineering degree with (Grade _____).

EXAMINATION COMMITTEE MEMBERS

1. Name: Dr Shahid Ikramullah Butt Signature:_____
2. Name: Dr Syed Omer Gilani Signature:_____
3. Name: Dr Emad Uddin Signature:_____

Supervisor's name: Dr Mohsin Jamil Signature:_____

Date:_____

_____ _____

Head of Department
(Dr Yasar Ayaz)

Date

COUNTERSIGNED

Date:_____

_____

Dean/Principal
(Dr Abdul Ghafoor)

DECLERATION

It is declared that the work entitled "**Proportional Resonant Control of Power Electronic Interface for Integrating Renewable Energy Sources**" presented in this thesis is an original piece of my own work, except where otherwise acknowledged in text and references. This work has not been submitted in any form for another degree or diploma at any university or other institution for tertiary education and shall not be submitted by me in future for obtaining any degree from this or any other University or Institution.

Rizwan Arshad
NUST201362034MSMME62113F

Acknowledgments

First and for most I am very thankful to the ALLAH almighty for giving me the opportunity and strength to complete my thesis.

I would like to thank my supervisor Dr. Mohsin Jamil, along with other committee members for evaluating this dissertation and for providing me with the requisite guidance and support, in order to successfully complete this work.

I am especially thankful to my parents, brothers, friends and other family members for their moral and financial support throughout my educational career.

I am also thankful to my fellows Usman Rashid, Muhammad Faheem Akram and Muhammad Waseem Akram who helped me in conducting the experimental testing and provided assistance.

Table 1: List of Symbols

List of Symbols	
CES	Centralized Energy System
DEG	Distributed Energy Generator
MC	Microgrid
IEEE	Institute of Electrical and Electronic Engineers
IGBT	Insulated Gate Bipolar Transistor
LCL	Inductor-Capacitor-Inductor
PWM	Pulse width Modulation
PID	Proportional-Integral-Derivative
PQR	Power Quality & Reliability
PZ-Map	Pole-Zero Map
RC	Repetitive Controller
RMS	Root Mean Square
SISO	Single Input-Single Output System
THD	Total Harmonic Distortion
VSC	Voltage-Source Converter
VS-PWM	Voltage-Source Pulse Width Modulation
PR	Proportional Resonant Controller
H(s)	Feedback Transfer Function
K_p	Proportional Gain
K_r	Proportional Resonant Controller Gain

Abstract

Power electronic converters are commonly used to interface renewable energy sources. There exist several topologies of these converters such as two level with LCL filter, multilevel, matrix and interleaved. This thesis focuses on two level LCL filter based topology which is commonly used in grid connected applications. To meet national international standards, there is requirement of suitable control strategy. It is an active area of research which has been investigated in this thesis.

Proportional Resonant Controller has been identified as a good candidate for said application. Its performance has been tested under different conditions especially system bandwidth. Moreover comparison with classical controller has been presented as well. The classical PI controller is found to be robust and able to provide high stability margins under varying load impedance however at the same time it has high harmonic content in the output current. Proportional Resonant controller is found to be adequate as it is able to provide low total harmonic distortion in the output current as compared to PI controller. Simulation results shows that proposed controller can provide better stability margins to the system, ability to attenuate grid harmonics and good robustness by carefully selecting the capacitor and inductor values in LCL filter as compared to PI controller.

Table of Contents

List of Figures

List of Tables

List of Journals/Conferences

- Mohsin Jamil, **Rizwan Arshad**, Usman Rashid, Yasir Ayaz and Muhammad Nasir Khan. Design and Analysis of Repetitive Controllers for Grid Connected Inverter Considering Plant Bandwidth for Interfacing Renewable Energy Sources, International Conference on Renewable Energy Research and Application (ICRERA), Pages: 468-473, 19-22 October 2014, Milwaukee, USA. ∗
- Mohsin Jamil, Usman Rashid, **Rizwan Arshad**, Yasir Ayaz and Muhammad Nasir Khan. Robust Repetitive Current Control of Two Level Utility Connected Converter using LCL Filter, Arabian Journal for Science and Engineering (AJSE), Volume 40, Issue 9 , pp 2653-2670, September 2015. ∗∗

∗ Attached in Annex 1

∗∗ Attached in Annex 2

Chapter 1
Introduction

1.1 Motivation and Introduction

Increased cost of conventional energy, emission of greenhouse gasses to the environment, the threats of depleting fossil fuel reserves and low efficiency of existing centralized energy systems (CES) are forcing the world to adopt renewable energy resources (RES) to fulfill its energy demand. Renewable sources and other distributed generators (DGs) can provide better efficiency, emission of harmful gasses can be limited and variable nature of renewable sources can also be managed within a microgrid. A microgrid is a mini grid within the main grid in which many electrical loads and generation systems including wind turbines, photovoltaic, fuel cell and many small thermal power plants combine/connect together and are controlled [1]. The concept of distributed energy generators (DEGs) and the microgrid (MG) concept are necessary for the understanding the working of the smart grid functions [2–5]. Distributed energy generators, energy consumers (or loads) and a main interface switch are the main constitutes of a microgrid. The concept of MG leads to better quality of power and increased reliability through islanding mood. It can minimize the line losses by alleviating or deferring the transmission system expansion. Greenhouse gasses can be limited to a great extent by incorporating renewable energy resources. Power electronic converters are used to interface the DEGs to the MG network and to facilitate the controlled operation of those units [6, 7]. A simple layout of microgrid is shown in Fig. 1.1.

Conventional energy sources like oil, coal and natural gas are rapidly depleting due to their increased demand. According to an estimate, energy demand throughout the world increased by 1.8% in 2012 [8]. Due to climatic variation throughout the world and limitation of fuel reserves, the world is moving towards renewable energy [9, 10]. To get maximum efficiency from these resources converters are being used for integrating these resources to the grid [11–13]. Power electronic converters are being used for exchanging and controlling power flow between the utility and DGs. They are normally used to connect these resources to the utility

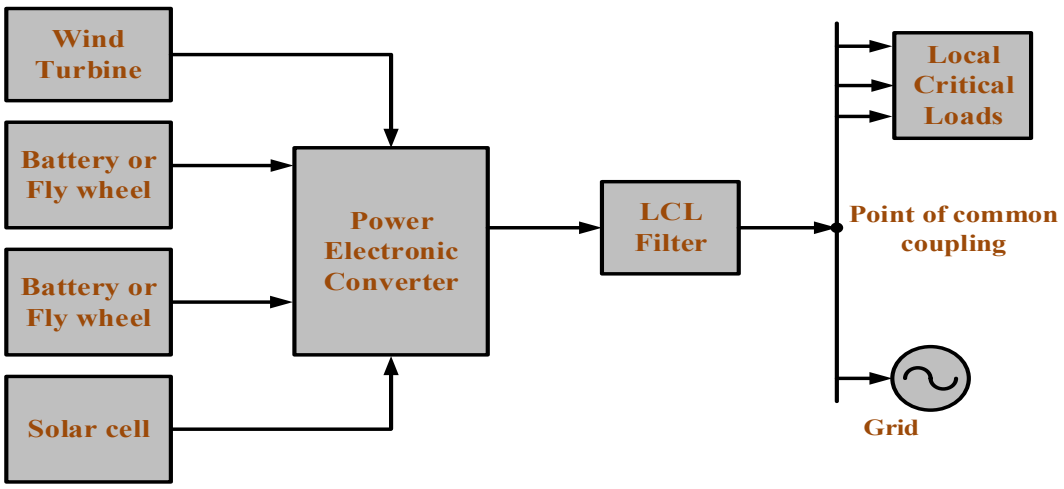

Fig. 1.1: A schematic diagram of a microgrid

Odd harmonic order n	**Percentage of fundamental(%)**
$n \leq 11$	4.0
$11 \leq n \leq 17$	2.0
$17 \leq n \leq 23$	1.5
$23 \leq n \leq 35$	0.6
$35 \leq n$	0.3
Even Harmonics	
$2 \leq n \leq 8$	1.0
$10 \leq n \leq 32$	0.5

Table 1.1: Allowable current distortion

or to supply local loads. These electronic converters control and improve the power quality by ensuring the total harmonic distortion (THD)in output current within the international standards [14–16]. The output current of the system designed in this thesis is tested against the harmonic limits of the IEEE standard 519-1992 (IEEE Standard 519, 1993) as shown in Table 1.1.

Today, several different types of power electronic converters are being used for interfacing renewable energy resources (RES) with the utility. This thesis research work is carried out by using the two-level bridge converter. It simple structure encouraged many researchers to use its different topologies. When MG is connected with the grid, each DEGs is supposed to maintain the synchronization with the grid and follow the set-points to avoid by the limits for current distor-

tion [17, 18]. Instead of two level converter, multilevel converters are also being used by the researchers [19–21]. These converters can provide better output but with complex control and increased cost of components. An interleaved converter topology can be used as an alternative to multilevel converters [22].

Voltage source inverters (VSI) are mostly used for obtaining AC from DC sources both in islanding and grid connected mode. A filter is essentially used between the VSI and grid for the the sake of reducing harmonics in the output current. An inductor in series can be used but it produces high voltage drop, very large in size and also unable to attenuate harmonics up to required limits [23]. Instead of using L filter now a days a lot of research is being done on high order filters especially LCL filter as it smooths the output current from the inverter [23] and meets the international standards of interconnection with grid at relatively small size as compared to L filter. This filter is commonly used these days because it gives higher attenuation of harmonics, cheap, small in size and have less weight as compared to L filter. This thesis focuses on the control of two level converter.

The research in this thesis is motivated by the work of *Mohsin Jamil* [24]. His research includes his novel idea of applying repetitive controller for two level converter and interleaved converter. However, repetitive controller requires excessive memory and increases computational burden on microprocessors. Therefore, PR controller is applied to address this problem for two level converter. A circuit diagram of the two-level three-phase pulse-width modulated (PWM) voltage source converter for utility interface investigated in this thesis is shown in Fig. 1.2. The parameters values are shown in Table 1.2.

In this circuit, the three-phase outputs of the converter are connected to the three phase utility system through an LCL filter. LCL filter prevents the entering of PWM switching frequency into the utility supply. When LCL filter is used, transfer function of two level converter becomes third order which results in complex control to deal with resonance produced by the filter. Due to low grid impedance value, there are chances that current harmonics can travel towards the converter which results can results in high THD value. This problem can be solved by increasing feedback controller gain at the expense of steady state error. This will be discussed further in the next chapters.

Zero steady stae error can be achieved if PI controller is used in synchronous (d-q) frame. However, a synchronous frame regulator is more complex as it involves

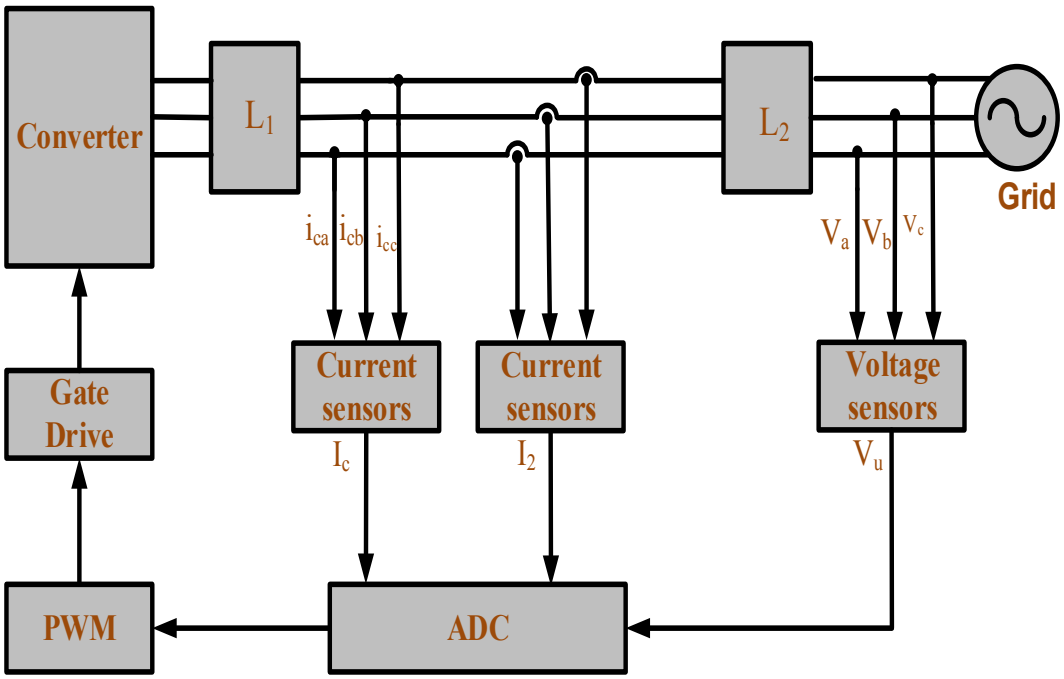

Fig. 1.2: Two-level power electronic converter interface with LCL filter

Table 1.2: System Parameters and Component Values for the Two-Level Utility Connected Converter with LCL Filter.

Parameters	Illustration	Rating values
V_u	Utility phase voltage	230 V(rms)
V_{DC}	DC link voltage	750 V DC
L_1	1^{st} inductor of filter	350 μH
L_2	2^{nd} inductor of filter	50 μH
C	Filter capacitance	160 μF
F_s	Switching frequency	8 KHz
F_g	Grid frequency	50 Hz
f_s	Sampling frequency	16 KHz
N	No. of samples per period	320
P_{inv}	Rated power	80 KVA

transformation, which can introduce errors if the synchronous frame identification is not accurate . The synchronous frame identification is normally based on a phase locked loop system, which may not be able to provide accurate phase information when the utility is non-ideal. An attractive approach to eliminate errors could be Proportional Resonant (PR) controllers, also known as generalised integrators. The PR controller works on the internal model principle, which introduces the mathematical model of sinusoidal reference along the open loop

path to ensure almost zero steady state error. However, the PR can act only on limited harmonics [25]. This will be discussed in detail in chapter 2. Zero steady sate error can be gained by using repetitive controller (RC) which works on the internal model principle.

In real system, THD could be any value and the output current will be more distorted, when THD is high and vice versa. It is desired to have pure sinusoidal current as much as possible without any distortions. The required low THD output current from converters can be achieved by implementing an effective control strategy. Conventional classical controllers have been widely used for utility connected converters . Simulation studies of the classical PI controller applied to the two-level system, have been carried out by the author to analyse performance and robustness of the overall two-level utility bridge system against different utility THD values. The classical PI controller was found not to provide output current as per the required standards when the utility voltage harmonic distortion is high. This happens because of low gain, higher steady state error and poor disturbance rejection of the PI controller at the utility harmonic frequencies. This will be further discussed in chapter 2.

There is a need of finding a controller which offers high gain at fundamental and other desired harmonics. To get higher outer loop gain and better disturbance rejection different controllers such as resonant control, optimal control can be found in the literature [26–28].Pros and cons are associated with every controller.

Many researchers used repetitive controllers (RCs) for limiting periodic disturbance present in grid connected inverters. RCs have the ability to provide better quality of current with less THD and higher gain at given 50 Hz frequency [29–32]. RCs are very sensitive to variation in parameters. The system become unstable if parameters or frequency is varied. Many researchers don't prefer to use RCs due to more memory requirement.

To ensure the maximum grid stability PI controller is used in this thesis to reduce the overshoot and for achieving better settling time. However, PI controller found not to follow a sinusoidal reference current and give poor disturbance rejection. A proportional resonance (PR) controller is used to overcome this problem. PR controller is selected due to its ability of offering infinite high gain at desired frequencies and almost zero gain at other undesired frequencies [33–36]. The aim of this study is to investigate the practical implementation and limits of two types

of controllers i.e. PI and PR controllers for current control of two level utility connected converter. Detailed simulations and theoretical analysis are given in this thesis by considering steady state error, transient response, utility impedance variations and limited filter bandwidth.

1.2 Objectives of Research

The objective was to improve the system performance by using PI and PR controller in terms of THD in output current and steady state error. Followings are the main objectives of the research conducted in this thesis.

- Develop appropriate computer simulation models (PWM switching model and linear transfer function model) for two-level converter using MATLAB/SIMULINK.
- Investigate the two-level converter with LCL filter and access the performance of the classical PI controller in terms of THD and steady state error requirement with different utility THD levels.
- Design and analyse proportional resonant control PR for two level converter by using inductor capacitor inductor (LCL) filter. Investigate the limits of performance of PR for this converter, particularly concerning system bandwidth by changing capacitance values of the LCL filter.
- Investigate stability limits, transient response and steady state error with respect to different parameters of PR.

1.3 Contribution of Thesis

Followings are the contributions of thesis.

- Two level converter with LCL filter is used for this study. The converter without any control technique exhibits enough gain margin (GM) and phase margin (PM) but posses very low bandwidth, which means it is unable to deal with higher order harmonics. So PI and PR controllers are used for

control purpose. The system's performance varies by varying the capacitance value of LCL filter and utility impedance (L_2). The effectiveness of the PR controller has been tested in the presence of different utility voltage harmonics and uncertainty in utility impedance. This issue has not been discussed in detail in the literature. PR controller is found to be a better candidate as it can provide better quality of output current by rejecting harmonics, better reference tracking, and enough plant bandwidth.

Followings are the contributions of thesis in terms of research publications.

- Mohsin Jamil, **Rizwan Arshad**, Usman Rashid, Yasir Ayaz and Muhammad Nasir Khan. Design and Analysis of Repetitive Controllers for Grid Connected Inverter Considering Plant Bandwidth for Interfacing Renewable Energy Sources, in International Conference on Renewable Energy Research and Application (ICRERA), 19-22 October 2014, Milwaukee, USA.
- Mohsin Jamil, Usman Rashid, **Rizwan Arshad**, Yasir Ayaz and Muhammad Nasir Khan. Robust Repetitive Current Control of Two Level Utility Connected Converter using LCL Filter, In Arabian Journal for Science and Engineering, 2015.

1.4 Thesis Organization

Chapter 2 presents a study of different current control methods such used for utility connected converters. Different damping methods which include active damping, passive damping and hybrid damping are presented to give a detailed overview of these techniques being used in utility connected inverters. Criteria for direct comparison and evaluation of current controllers (PI & PR) performance are defined.

Chapter 3 presents the derivation of single-phase equivalent circuit. The converter's block diagram is presented which is used for designing and analysing of the control system for two level converter. The design of classical controller and PR controller is briefly explained.The PR is adopted because it can offer infinite gain at desired harmonics simultaneously and can address the limitations of other control techniques.

Chapter 4 discusses the analysis of a PI and PR controller. Simulation results are shown in this chapter to explain the results in terms of stability, steady state error and transient response of the given system.

The final chapter presents the conclusions of the research and recommendations for further work.

Chapter 2

Review of Various Control Techniques for Interconnecting Renewable Energy Resources with the Grid

2.1 Introduction

This section includes the review of research articles related to the different control strategies employed for utility connected converters. There exist different structures (e.g. Fig. 2.2, Fig. 2.3, Fig. 2.4 and Fig. 2.7) of the two-level converter with output LCL filters. In this section, the common structures of the two-level converter based upon single and double feedback loops with output LCL filter are reviewed.

2.1.1 Controller Objectives

The controller to be designed for grid has to control:

- Power delivered to the grid (Active or real power)
- Reactive power transfer
- DC voltage
- High quality of output current
- Synchronization with grid
- Local voltage
- Frequency regulation
- Total Harmonic Distortion

Conventional classical controllers (P/PI/PID) have been widely used. However, the quality of output current from these controllers is poor due to low loop gain at fundamental frequency and desired frequencies which results high THD in output. The limitations of classical controllers are being overcome by alternative control techniques such as proportional resonant (PR), deadbeat, repetitive control (RC) and many others.. Moreover, modifications in existing control structures can also help to address these limitations. This chapter discusses different current control techniques and structures used for utility connected converters.

2.1.2 LCL filter: A better Choice

LCL filter when compared with L and LC filter gives better performance [37]. When converter is designed by using LC filter, resonance frequency of the filter is determined by utility impedance. This makes life difficult and the filter resonance cannot be dampened. In case of high rating devices, the losses in the inductors cannot be ignored. Moreover, larger inductors are more expensive than the smaller ones. LCL filter has advantage because it ensures small inductor size, less losses and reduced size of the whole system. Thus cost of whole system decreases. In Fig. 1.2 switching frequency, max. current ripple and DC voltage decide the size of inductor L_1. The capacitance value is such that its impedance value is lower than the value inductor L_2 at switching frequency. The value of L_2 in filter is actual value not utility impedance. The importance of the inductor L_2 is due to three reasons:

- It ensures filtration of current harmonics.
- It makes the controller performance less sensitive to utility impedance variations.
- It facilitates wireless paralleling of multiple systems.

This LCL filter based configuration, requires a suitable control technique to handle the filter resonance problem. The purpose of the controller is to achieve low output current THD with zero steady state error. In other words, a better disturbance rejection and good tracking is desirable.

2.2 Active Damping

Active method uses a closed loop for controlling current of the converter [38–41] to suppress resonance oscillation. Active damping uses current sensors and control techniques to reduce DC current entering into the grid. Active damping provides flexible control and lossless damping. Output of active control method contains a mixture of DC and AC current and involves limitation i.e. current controller bandwidth due to stability margins. By using current control it is quite possible to reduce DC current component in the output if DC component can be measured.

2.2.1 Pole placement and PR controller Method

The constant errors at specific frequency values can be fully attenuated by the use of PR controller as it offers infinite gain at certain values of frequency and provide improved quality of current that can be fed to the grid [42, 43]. For a stable system, proportional resonant controller are often found difficult to design as it is a multi-order system. If one is using an LCL third-order filter plus PR controller then the design will becomes much complicated for such systems [44]. To deal with such systems a PR controller is presented in [42] with capacitor's current as feedback and based on root locus theory. In which one can select parameters of PR controller from the root locus plot keeping in view the system's stability and its dynamic response. Based on the research by authors of [45] a control design strategy using stationary frame method is proposed in [46]. To measure the the system stability and robustness, parameters of controller and parameters of LCL filter are analyzed in discrete domain. In this analysis a PR controller was proposed by using pole placement method. This proposed design was verified by a 10 kW prototype. PR controller is able to offer an infinite gain at the frequency of W_h and shift of 180^0 in phase. As it is multi proportional resonant so infinite gain is not required for system stability. Hence ideal PR controller is commonly changed into single PR which is used practically [44]. Equation (2.1) gives the transfer function of PR controller.

$$G_{PR}(S) = K_p + \frac{2K_i\omega_c s}{s^2 + 2\omega_c s + \omega_h^2} \tag{2.1}$$

Approximately there was zero static error of closed loop system by PR controller.

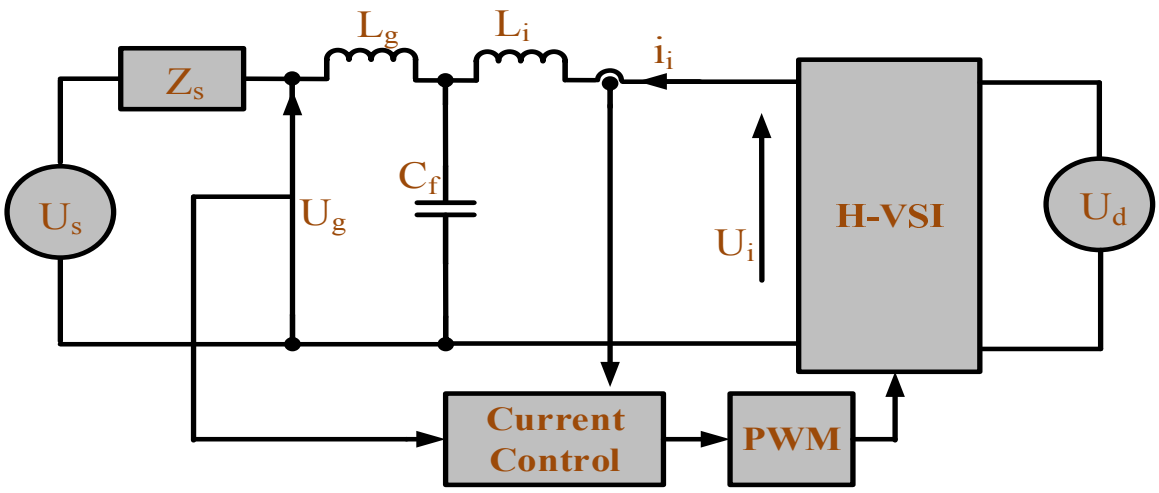

Fig. 2.1: Schematic diagram for LCL filter for PR controller [44]

Different impacts including the impact by parameters of PR regulator, impact of digital control delay and impact by LCL filter on root locus were discussed and their results have been explained by diagrams in [44]. Experimental verification was carried out by A 3 kW inverter with LCL filter, as shown in Fig.2.1.

Parameters were selected from the research of *Marco et.al* [47] and their values are given as L_g=1.8mH, L_s=2mH, C=4.7μF and R=2.2Ω. The poles of system were placed in the left half plane and then enough damping of poles was maintained to minimize the effect of resonance and to ensure the stability. Poles should be kept away from the imaginary axis to ensure the better stability. For large systems, gain at ω_h and integral gain K_i should also be large as long as the system remains stable. The selected roots of closed loop transfer function are:

$$\begin{aligned} P_{1,2} &= -4922 \pm 26089j \\ P_{3,4} &= -3479 \pm 10059j \\ P_5 &= -2556 \\ P_6 &= -0.0045 \end{aligned}$$

Another important result can be visualized from the graphs of [48] i.e. the proposed PR controller exhibits more robustness than conventional PI controller if voltage feed-forward method is adopted [49]. By using voltage feed-forward, the controller can reject the grid disturbances better and can better adopt to power range. When the grid was feeding by 3 kw power and PI controller was used,

THD was approximately 8% however using feed-forward with PI controller THD was improved to 4.3%. THD was further improved to 4% when grid fed power was 5-10 kW. So PR controller can give the same results as PI+FF over a wide range of power.

2.2.2 Full-feed-forward method

Research on feed-forward schemes for inverters with L filter has been widely explored in the literature [50, 51]. but research on feed-forward schemes for LCL filter was less as compared to L filter. The authors in [52] extensively studied full feed-forward method for LCL filter. Active damping with capacitor current feedback proposed in [53] is used in [52] for its implementation. The experimental results obtained from this scheme are appreciable. Simulation results showed that total harmonic distortion (THD) was 4.6%. The results showed that the full feed-forward scheme can minimize the grid current harmonics effectively.

2.2.3 Single Loop Feedback Strategy

Hussein [54] and others [55] proposed a single feedback loop structure for a voltage source PWM converters shown in Fig. 2.2 by using L_1 and I_1 as the only feedback control signal. This results in a stable and simple system, which requires only one measurement of each phase current (I_1). For this structure, equations (2.2), (2.3), (2.4) give $G_1(s)$ and $D_1(s)$ as plant transfer function and disturbance transfer function.

$$G_1(s) = \frac{1}{(L_1L_2C)s^3 + (K(s)L_2C)s^2 + (L_1 + L_2)s} \tag{2.2}$$

$$D_1(s) = (L_1Cs^2 + K(s)Cs + 1) \tag{2.3}$$

The input-output relation of this structure is given by equation (2.4)

$$I_2 = \frac{K(s)G_1(s)}{1 + K(s)G_1(s)}I_{ref} - \frac{G_1(s)}{1 + K(s)G_1(s)}D_1(s)V_u(s) \tag{2.4}$$

The disadvantage of this structure is that the plant (two-level converter and output LCL filter) $G_1(s)$ and $D_1(s)$ are functions of controller $K(s)$. If the controller $K(s)$ has to be designed to improve reference tracking and disturbance rejection,

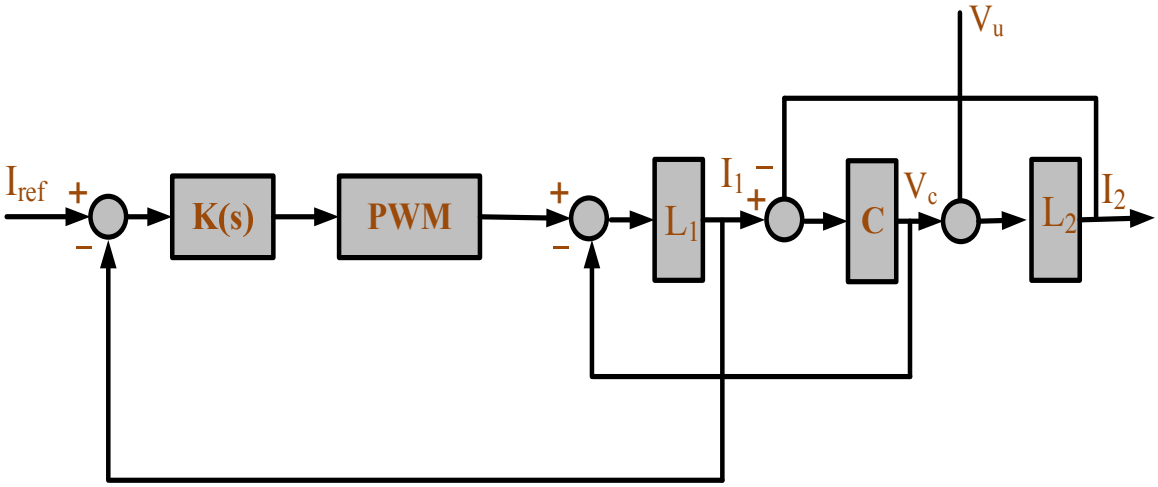

Fig. 2.2: Single loop feedback structure of I_1 [54]

this will result in a change in $G_1(s)$ and $D_1(s)$, which complicates the controller design. Also, it is not able to track reference and gives poor disturbance rejection.

Utility voltage V_u forms a source of disturbance to the system. Ideally, this disturbance can be rejected by implementing a feed forward loop of exactly the same shape as the utility disturbance transfer function $D_1(s)$. In reality, however, it may be difficult to apply the first and second derivatives of the utility voltage V_u, due to noise amplification problem. Derivatives are obtained by an offline calculation using a well-known nominal value (230 Vrms) of the utility voltage [54, 56].

2.2.4 Two Loop Feedback Strategy

Abusara[56] used a two loops feedback system with the output current as the outer loop and the capacitor current as the inner loop (Fig. 2.3). Use of only output I_2 of LCL filter makes the system unstable. To make the system stable I_c or inductor current L_1 [37, 56, 57] should be used. Using output current I_2 and capacitor current I_c, equations (2.5), (2.6) give the plant transfer function $G(s)$ and disturbance transfer function $D(s)$.

$$G(s) = \frac{1}{(L_1L_2C)s^3 + K_cL_2Cs^2 + (L_1 + L_2)s} \tag{2.5}$$

$$D(s) = L_1Cs^2 + K_cCs + 1 \tag{2.6}$$

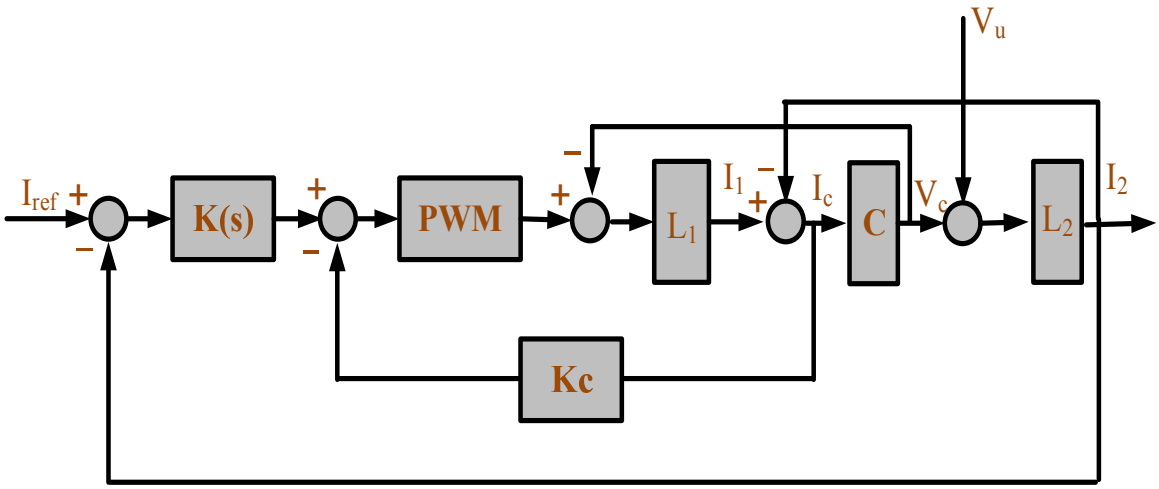

Fig. 2.3: Double feedback loop structure of I_2 and I_c [56]

The input-output relation of this structure is given by equation (2.7)

$$I_2 = \frac{K(s)G(s)}{1 + K(s)G(s)} I_{ref} - \frac{G(s)}{1 + K(s)G(s)} D(s)V_u(s) \tag{2.7}$$

$G(s)$ and $D(s)$ are independent of the controller $K(s)$ but dependent on inner loop gain K_c which makes the design of a controller easier. The voltage feed forward is implemented by having fundamental voltage and its derivatives.

2.2.5 Split Capacitor

Another interesting structure is proposed by *Guoqiao* et al. [58]. This study focuses on dividing LCL filter into two halves connected in parallel (Fig. 2.4). The current after first capacitor is feedback The authors used the sum of the utility current and a part of the capacitor current as feedback. One can overcome the resonance problem and also can reduce the transfer function to first order by suitably selecting the capacitor values. It provide better output loop gain which results in improved disturbance rejection. Practically it is difficult to find capacitors with the desired values.

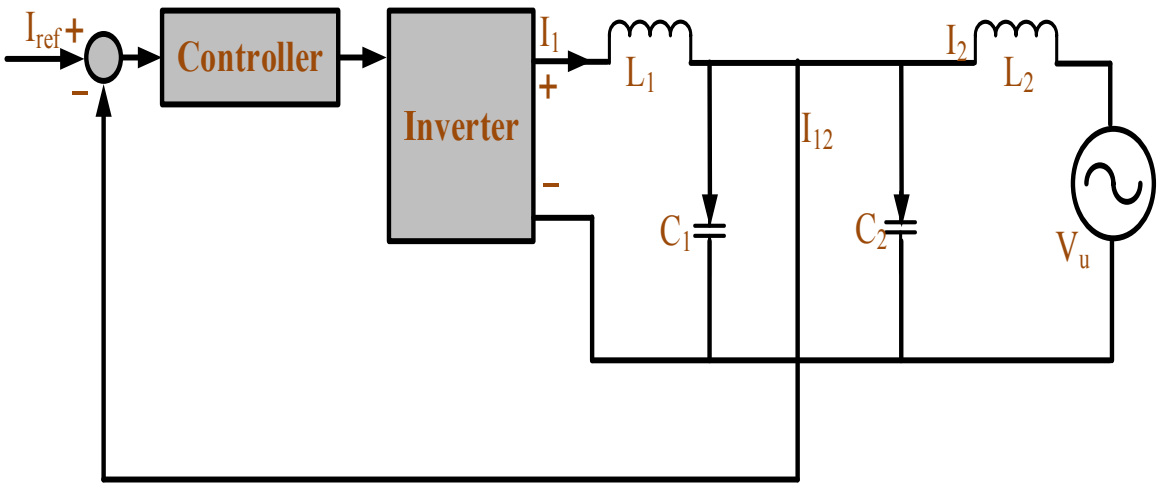

Fig. 2.4: Block diagram of LCCL based control structure proposed by (Guoqiao et al., [58]

2.3 Passive damping

Passive methods are reliable and easy to implement. A resistor is added in series with the capacitor to make passive damping [59]. Passive damping unable to reject higher order harmonics with high power loss. For application in high power, simple series resistor method is not sufficient enough. To make the system efficient, more damping circuits for line-side filters are tested in [60]. Requirement of high quality power and high attenuation leads to a multi-level inverter which not only raises size of inverter and cost but also reduces system's efficiency. Furthermore, for such multi-stage inverter structure, optimization problem becomes highly complex. So there is a need of much more improved and optimized solution.

2.3.1 Split resistor strategy

In grid connected converters power loss occurred in LCL filter due to passive resistors adds up to considerable portion of total power loss. Based on the stored energy some efforts have been made to optimize the design procedure in [61] but however power loss in filter was large. A shunt hybrid damping scheme $C_1 - C_d - R_D$ is adopted with both active and passive strategies in [62]. It was supposed that design of LCL filter will not vary significantly whatever the

damping type is used [63]. The per phase equivalent diagram is shown in Fig.2.5. In grid connected mode, transfer function which effects the closed loop is given as

$$G(s) = \frac{1}{s^3 L_1 L_2 C + s(L_1 + L_2)} \tag{2.8}$$

The frequency at which resonance will occur is given by the following equation

$$\omega_r^2 = \frac{1}{L_p C} \tag{2.9}$$

where L_P lumped capacitance is given as

$$L_p = \frac{L_1 \times L_2}{L_1 + L_2} \tag{2.10}$$

It was supposed that L_1 and L_2 are related by following equation

$$L_1 = \alpha_L L_2 \tag{2.11}$$

then ω_r is given as

$$\omega_r^2 = \frac{1}{C \times L \frac{\alpha_L}{(\alpha_L+1)^2}} \tag{2.12}$$

The value of capacitance depends on the resonance frequency ω_r and the ratio of L_1+L_2. Active damping can be used to suppress the resonance peaks if the ω_r is within the compliance of closed loop bandwidth. But if ω_r is not within the range then passive method using resistors is the solution. Active damping offers less power loss at full load. Passive methods must be used for applications in which the inverter is switched off but the filters are still connected to the utility grids. If harmonic occurs in voltage/current at resonance frequency it can cause instability. From the Fig.2.5 it is obvious that total inductance is the sum of L_1 and L_2 and capacitance is the sum of C_1 and C_d. Now it was supposed that $C_d = \alpha_c C_1$ where α_c is a numerical value selected. To visualize the effect of α_c on the damping, transfer function is given given in following equation.

$$G(s) = \frac{P(s)}{L(s)} \tag{2.13}$$

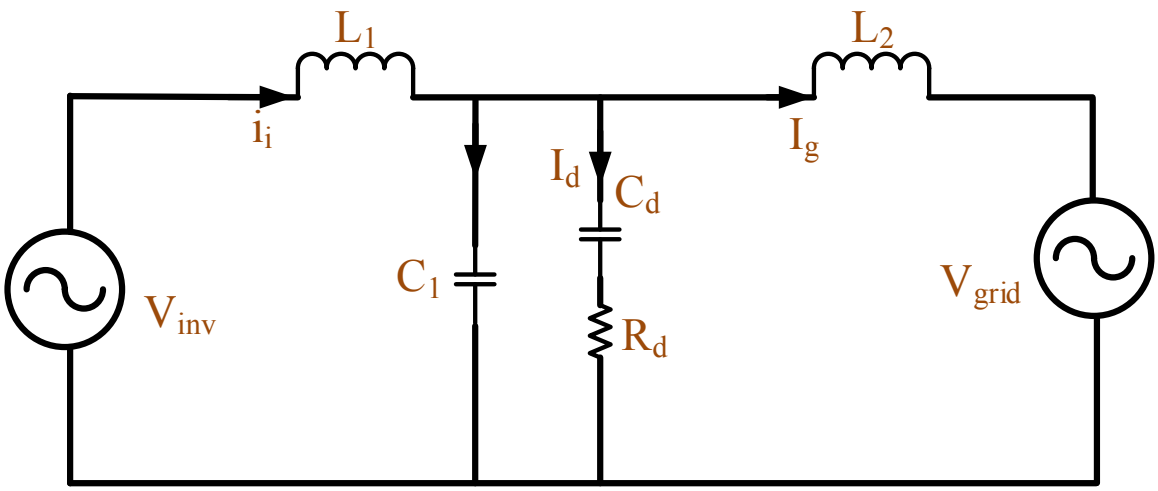

Fig. 2.5: Per phase model of split capacitor resistor strategy

where

$$P(s) = (sL_2 + s^2 L_2 C_d R_d)$$

$$L(s) = s^4 L_1 L_2 C_1 C_d R_d + s^3 L_1 L_2 (C_1 + C_2) + s^2 C_d R_d (L_1 + L_2) + s(L_1 + L_2)$$

R_d was calculated by relation

$$R_d = \sqrt{\frac{L}{C}} \tag{2.14}$$

For evaluation of results from the experiment, values used for LCL filter were L_1=3.385mH, L_2=3.439mH, C_1=8μF C_d=8μF, R_d=25Ω. Three phase inverter was used for conducting open loop tests at switching frequency of 10 kHz and DC bus voltage was 600 V. The experimental results shows that the ripples in the short circuit output current in stand alone mood is within the distortion limits. The drawback of this technique is that LCL filter was used only to attenuate high order harmonics and adequate filtering range was kept above the resonance frequency i.e. 1 kHz. The waveforms of output current contains lower order harmonics as converter is operating in open loop conditions. So the total harmonic distortion in output current exceeds the defined limitations. and to suppress these low order additional control techniques are required.

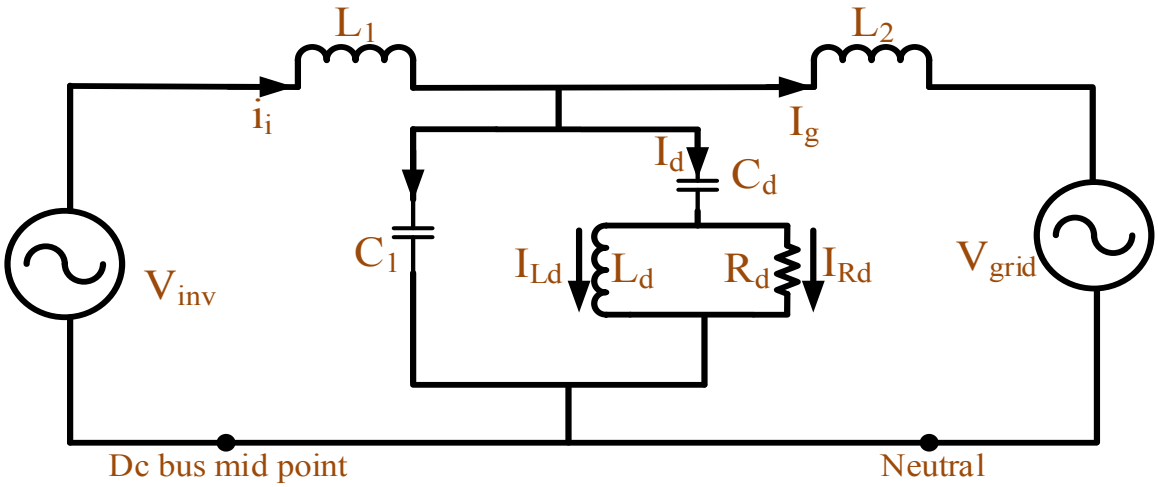

Fig. 2.6: SC-RL damped LCL filter

2.3.2 SC-RL damping for LCL filters

The control of passive damping is less complicated and is highly reliable [62,64,65]. *Channegowda* and *John* [62] did extensive research on (SC-R). They estimated power loss in resistor yet there work was limited to a few kilowatts of power level as losses due to passive resistor would be increased rapidly if power level is increased further. Split capacitor resistive-inductive (SC-RL) strategy adopted in [66] presents a substitute to resistive damping and to the strategy analyzed in [62]. For a given level of power quality corresponding power loss in resistive damping is analyzed in [66]. The authors in [62] made assumptions by computing power loss in worst case of switching ripples but in [66] more accurate values were used for calculating power loss happened due to switching ripples by developing a model of LCL filter in state space and and verified the values by experimental results. The configuration shown in Fig.2.6 is used. Middle point of DC bus is connected to the middle point of filter capacitors. For the sake of simplicity, ideal filters are shown only and damping components are omitted. The reason of selecting this configuration is because it provides current ripples in worst case and highest power losses in damping resistor as inter-connection switching ripples can circulate through neutral point.

I_g, I_i, V_c, V_d and I_{Ld} were chosen as state variables and based on these variables

following system was obtained.

$$\dot{x}(t) = \bar{A}x(t) + \bar{B}u(t) \tag{2.15}$$

$$y(t) = \bar{C}x(t) + \bar{D}u(t) \tag{2.16}$$

Their corresponding matrices are given in [62] where V_i and V_g are the inputs to the model and I_{RD} was chosen to be the output so that power loss in damping circuit can be calculated. LCL filter exhibits both series and parallel resonance. Series resonance should be considered for damping analysis as it can cause large current to flow if left undamped. To study the series resonance damping, transfer function used was

$$G(s) = \frac{V_C(s)}{V_I(s)} \tag{2.17}$$

where

$$V_C(s) = R_d C_d L_2 L_d s^3 + L_2 L_d s^2 + R_d L_2 s$$

$$V_I(s) = R_d L_1 L_2 C_1 C_d L_d s^5 + L_1 L_2 (C_1 + C_d) L_d s^4$$
$$+ R_d [L_1 L_2 (C_1 + C_2) + L_d C_d (L_1 + L_2)] s^3 +$$
$$(L_1 + L_2) L_d s^2 + R_d (L_1 + L_2) s$$

A higher order LCL filter with SC-RL damping method shown in Fig.2.6 needs many complicated parameters to arrive at optimal values and it is possible that this will provide an appropriate design. In [62] damping elements are added in steps to LCL filter for achieving optimal solution. The aim of adding every new element was to maintain *quality factor* and *total power loss* as low as possible. C was divided into parts C_1 and a series combination of C_d with L_d and R_d in parallel was made to obtain SC-RL damping. While selecting all these values of parameters effect of switching frequency, resonance frequency, inductance and capacitance values was also under consideration. DC bus voltage for inverter was 800V and switching frequency was 9.75 kHz. The parameters for LCL filter can be selected from numbers of methods [67–70]. In [66] LCL parameters were selected based on the study of *John and Channegowda* [62]. For low vales of L_1 and L_2, loss due to ripple current prevailed and if values are selected larger than power loss decreases. So a compromised value 0.02 pu was selected. Value of C was decided on the basis of ω_r which is based on fundamental frequency and

switching frequency. For best choice one should select ω_r well differentiated from fundamental and switching frequency.

After the selection of LCL filter parameters, values of C_1, C_d and R_d were found in similar way as *Channegowda and John* did in [62]. Quality factor QF and total power loss P_T lead to the selection of L_d value. Using the expressions given below a graph was plotted between total power loss damping impedance factor K_{L_d}.

$$P_{f_u} = \frac{C_d^2 R_d}{K_{L_d}^2 - 2C_d R_d K_{L_d} + (1 + C_d^2 R_d^2)} \tag{2.18}$$

$$P_{r_i} = (i_{R_d}, rms)^2 R_d \tag{2.19}$$

$$P_t = P_{f_u} + P_{r_i} \tag{2.20}$$

Where P_{f_u} is power loss due to fundamental component of current, P_{r_i} is power loss due to ripple component of current and all these values are in per unit system. Curve of graph shows that for P_T, value of $K_{L_d} = 20$ is best choice. It was supposed that if ideal LCL filter is changed by introducing passive damping component and K_{L_d} is equal to 20, resonance frequency ω_r will not vary. So one should tune K_{L_d} numerically. Bode plot obtained from transfer function V_C/V_i (2.17) was used to tune K_{L_d} numerically.

To study the effect of proposed scheme experimentally, an inverter was designed in the laboratory. The curves showed that experimental damping curve is better than theoretical prediction.

2.3.3 Two Loops Feedback Structure with Passive Damping

Another structure proposed by the same authors *Guoqiao et al.* [71] suggested the use of both feedback currents i.e. I_1 through the L_1 and I_2. The feedback from both the currents are feedback to control the converter. This method involves an extra current sensor, compared to *Hussain* [54] and *Guoqiao et al.* [58]. Moreover, it also requires an additional resistor in series to the capacitor shown in Fig. 2.7. However, in high power applications, a damping resistor will be subject to losses and efficiency of the system would be affected [72]. Alternatively, active damping could be used, which requires the same number of sensors as used by *Abusara* [73] and discussed earlier. Active damping is obtained through the product of

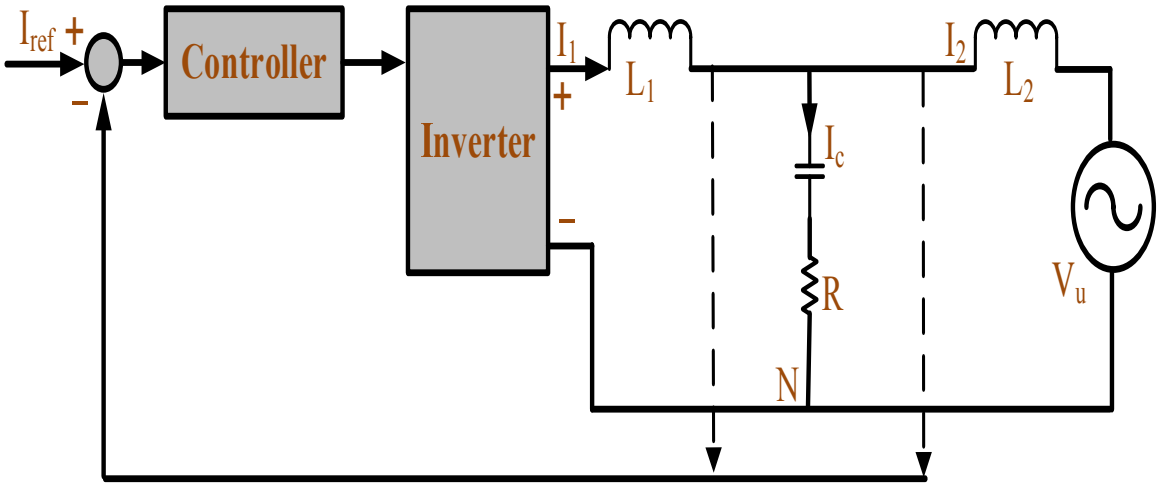

Fig. 2.7: Block diagram of two loops feedback structure with passive damping proposed by *(Guoqiao et al.)*[71]

the capacitor current ($I_c = I_1 - I_2$) and gain K_c. This structure can handle larger utility harmonics very well compared to the earlier schemes.

The structure used by *Mohsin* in [24], as shown in Fig. 2.3, is selected for further investigation. The two-level converter based on this structure is available in the laboratory. This structure involves the use of the output current and inner loop capacitor current as discussed earlier.

2.4 Hybrid Damping

An effort is made to combine benefits of both active and passive methods in [74] to ensure stability margin, dynamic response and damping performance and named it as hybrid damping. In the proposed approach a four-state filter structure is used which had fewer system losses as compared to conventional passive method and active algorithm. Existing active damping methods need feedback loop but hybrid damping needs no additional sensor and feedback signal for damping performance. A parallel combination of resistor and capacitor has been proved more adequate and useful than series combination. Passive part of hybrid damping used RC parallel method and for active damping used a four state RC-parallel passive filter model. Furthermore, state space and proportional integral technique with improved stability margin is used for current control [74]. There were two main reasons of choosing RC parallel damping technique in this paper.

Table 2.1: FFT's of higher order harmonics

Filter name	FFT(% of fundamental)				
Frequencies	f_s	$2f_s$	$3f_s$	$4f_s$	$5f_s$
LCL	0.08	0.01	0.00	0.00	0.00
Hybrid	0.09	0.04	0.01	0.00	0.00

- At lesser losses, required damping performance could be achieved at fundamental and switching frequency.
- In addition to damping resistance (R_d), using C_f/C ration provides another freedom of improving damping performance.

From the table 2.1 it is obvious that at switching and higher order frequencies performance of LCL filter is superior than damped LCL filter. For observing significant difference one must use higher values of R_d or C_f this happens because parallel damper offers a zero at higher frequencies. So higher values of C_f or R_d affect distortion of desired harmonics. To show that proposed scheme is more effective than conventional LCL filter method, the transfer function $(i_{L1}(s))/i^*_{L1}(s))$ used is same for both methods. While deriving the transfer function K_p has been supposed to be in the inner current loop. The earlier studies shows that by increasing the value of k_p, stability decreases. To check the stability issues, same experiment is done with hybrid system in [74] and the results showed that there has been much improved phase margin as compared with existing LCL filter with only active damping even for higher values of k_p. It is also of worth noticing that increasing the passive damping or higher the ratio C_f/C gives wider range of stability. R_d's value can be changed to obtain the similar results. It is obvious from the graphs of [74] that hybrid damping tracks the reference current much faster or it has better transient response as compared with response of active damping. It is very difficult to achieve high system bandwidth with active damping because system becomes unstable when K_p exceeds 56 but contrary to that hybrid solution provides much wider bandwidth and using hybrid solution system degrades only for $K_p > 100$. A suitable value between system losses and dynamic performance is required because increasing passive damping increases system losses but on the other hand provides higher controller gain or bandwidth. To decide trade-off between dynamic performance and power losses depends on practical application. Practical application of LCL filter is increasing rapidly due to its

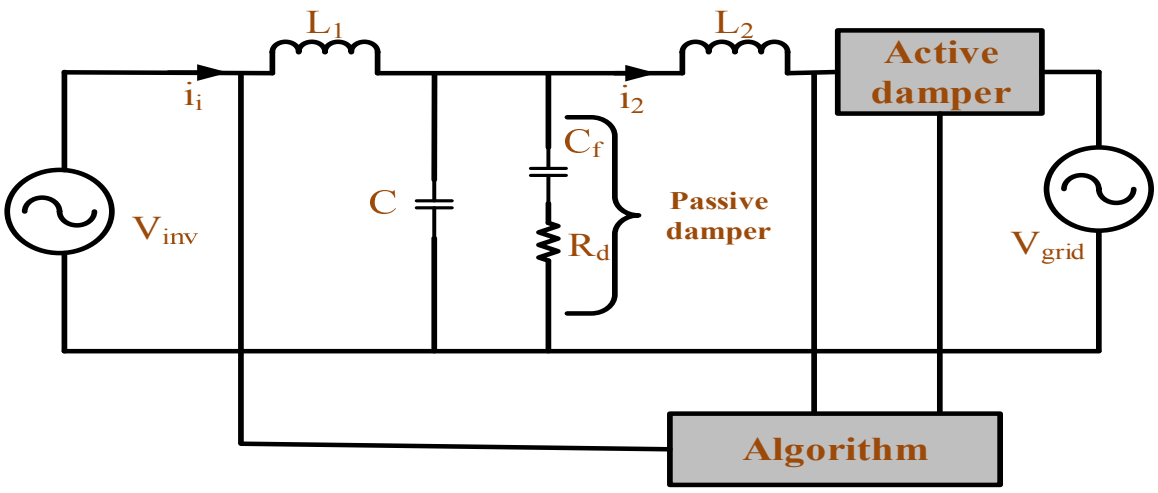

Fig. 2.8: Hybrid Damping

smaller size and better performance of harmonics rejection which are injected into the grid. However, at resonance frequency LCL filter offers zero impedance so an oscillation will be produced in the control loop due to this resonance peak. In order to minimize resonance caused by LCL filter active, passive and hybrid methods are suggested so that performance of the grid connected system can be enhanced both in high and low frequency ranges. System becomes more complex in active damping whereas circuit losses dominate in passive damping so hybrid damping can provide an optimal balance between them. While designing the control strategy of LCL filter for grid connected inverters following rules must be kept in mind:

- Circuit power losses should be minimum
- Lower system complexity
- Overall system cost should be minimum
- Reduced number of current sensors/AD sensors
- Higher stability and reliability

2.5 Comparison criteria for evaluating the current control techniques

The performance criterion for the current controllers is the quality of the current waveforms they produced. For direct comparison of different current controllers a criteria must be defined. The lowest distortion index indicates the highest quality waveform. Two complement indices are defined as total harmonic distortion and percentage RMS current error based on the steady state performance requirement. Additionally, transient performance requirement is also important which is briefly discussed here. Other than steady state and transient performance requirements, losses also become important for utility connected converters especially while performing power flow control.

2.5.1 Total Harmonic Distortion

The power supplied by distributed energy systems can severely affect the power regulation and consumption. The amount of distortion in the line current waveform is quantified by means of an index called the total harmonic distortion. Non-linear loads causes the distortion of waveform which leads to creation of harmonics. These harmonics are the reason behind the interference problem in communication and also deteriorate power distribution and transmission. They are also responsible for insulation break up in motors and transformers. So its crucial to know the THD in the system. The sum of all the harmonic present the output waveform of a system is known as total harmonic distortion. It is the sum of the Fourier (harmonic) components of the fundamental frequency current as a percentage of the fundamental component as given in the equation 2.21. In simple words, the extent to which a sine wave deviates from its pure sinusoidal value is called total harmonic distortion. Zero harmonics are present in ideal sine wave. By obtaining the THD in the current waveforms generated by different current controllers, the performance of the current controllers can be compared with each other and with the current harmonic limit standards such as ANSI/IEEE Standard 519-1992 mentioned in table 1.1 in chapter 1.

$$THD = \frac{\sqrt{V_2^2 + V_3^2 + V_4^2 ... V_n^2}}{V_1} * 100\% \tag{2.21}$$

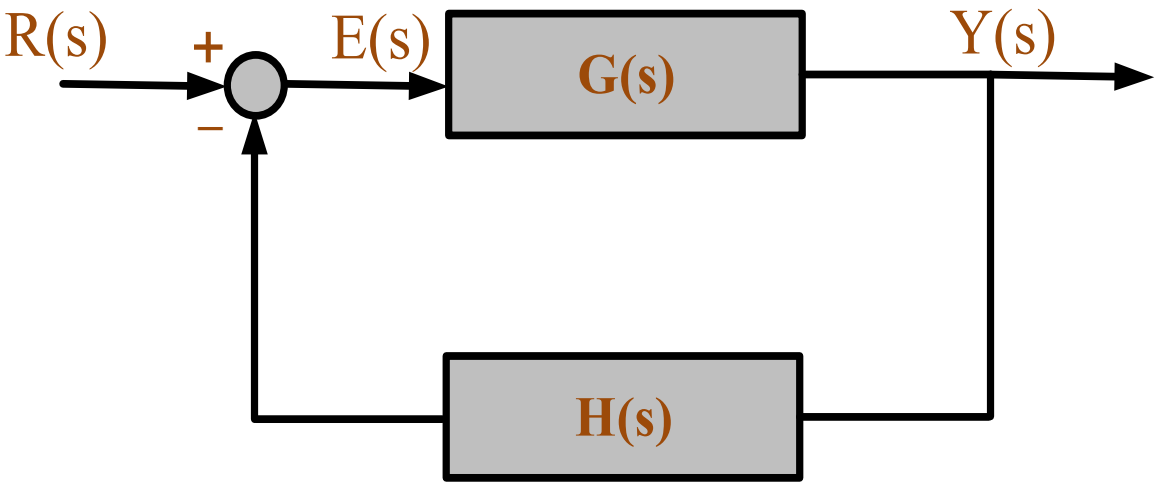

Fig. 2.9: Closed loop system

The THD in the line current is defined as:

$$THD = 100 \times \sqrt{\sum_{k \neq 1} \frac{I_{sh}}{I_{s1}}} \tag{2.22}$$

Where, I_s1 is the fundamental component (f_1) and (I_sh) is the component at the $'h'$ harmonic frequency.

2.5.2 Steady State Error

It can be defined as the error in stable system between the command and the response of a stable when time approaches to infinity. For measuring steady state error system must be stable. So stability of specific system must be checked/ensured before checking the steady state error of that system. If the system is fed by unity feedback then steady state error can be estimated from the open/closed loop transfer as given in Fig. 2.5.2. The equations 2.23, 2.24 and 2.25 can be used to calculate steady-state error.
Step Input$(R(s) = 1/s)$:

$$e(\infty) = \frac{1}{1 + \lim_{s \to \infty} G(s)} = \frac{1}{1 + K_p} = K_p = \lim_{s \to \infty} G(s) \tag{2.23}$$

Ramp Input ($R(s) = 1/s^2$:

$$e(\infty) = \frac{1}{s \lim_{s\to\infty} G(s)} = \frac{1}{K_v} = K_v = \lim_{s\to\infty} sG(s) \tag{2.24}$$

Parabolic Input ($R(s) = 1/s^3$):

$$e(\infty) = \frac{1}{s^2 \lim_{s\to\infty} G(s)} = \frac{1}{K_a} = K_a = \lim_{s\to\infty} s^2G(s) \tag{2.25}$$

2.5.3 Transient response

As the name is indicating that transient means change. This change occurs mainly after two conditions which are given below.
Condition one : when a system is switched on.
Condition second : when sudden changes in a system.

In addition to steady state performance requirements, in terms of better disturbance rejection and low steady state error, it is essential to have an accurate and fast transient response as well. Reduced overshoot and settling time without any oscillations in any controller design is always desired. It becomes more important in converter control when operating into a distorted supply. Over currents and overshoots are most likely to happen in presence of unbalance supply. Normally suitable protection schemes are employed for this purpose.

2.5.4 Plant Bandwidth

The plant bandwidth plays a vital role in the design of any feedback controller. Its importance is more for PR based systems because it is required to provide higher gains at desired frequencies. One of the stability conditions for PR based system is that the plant with a basic feedback controller without PR controller should be stable. Switching frequency and resonant frequency are essential for determining the bandwidth of the system. The capacitance values of the LCL filter determines the resonant frequency of LCL filter. In this way, the designer could have an idea about achievable harmonic compensation by the PR controller and required component values [75]. As a rule of thumb, the switching frequency should be at least two times the resonant frequency for effective harmonic compensation around the switching frequencies.

Chapter 3
Derivation and modeling of Two level Converter

This chapter describes a brief modeling and derivation of two level converter.

3.1 Derivation of Transfer Function

Abusara in [56] used a two loops feedback system for two level converter with the outer loop current I_2 and inner loop capacitor current I_c as shown in Fig.1.2. The control of this structure is investigated here. Single phase circuit as shown in Fig. 3.1 is used for analysis and designing of the system. The voltage difference between neutral and DC link is represented by V_{gn} in Fig. 3.1

V_{gn} can be represented by the following equation:

$$V_{gn} = \frac{V_{ag} + V_{bg} + V_{cg}}{3} \tag{3.1}$$

where V_{ag}, V_{bg} and V_{cg} are phase voltages of phase a, b and c w.r.t ground. By considering the single-phase equivalent circuit for the utility connected voltage

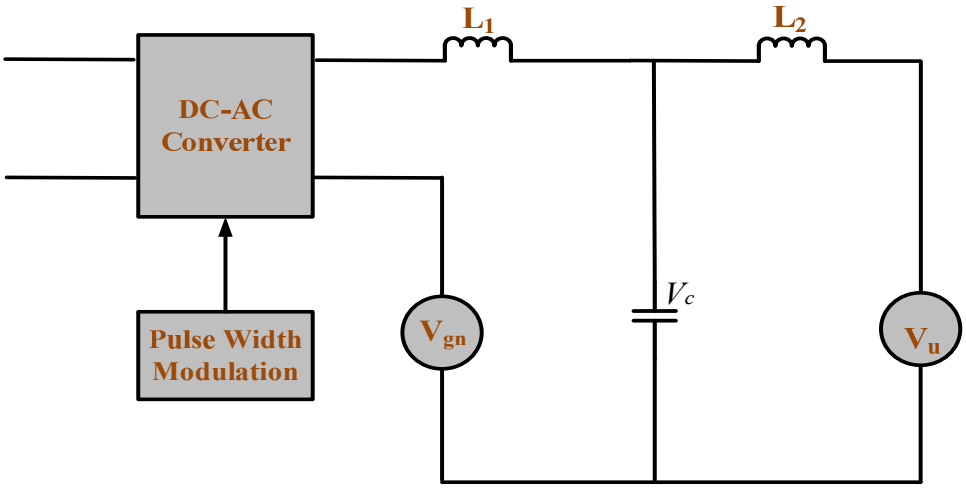

Fig. 3.1: Single-phase equivalent circuit of the two level converter.

source converter without phase interaction term, the following equations can be developed.

$$V_{in} - V_c = L_1 \frac{dI_1}{dt} \tag{3.2}$$

$$I_c = I_1 - I_2 \tag{3.3}$$

$$I_c = C \frac{dV_c}{dt} \tag{3.4}$$

$$V_c - V_u = L_2 \frac{dI_2}{dt} \tag{3.5}$$

The expression of the output current, I_2, in s-domain is derived and shown below. Substituting equation (3.4) in (3.3) and after differentiating, equation (3.6) is obtained.

$$\frac{dI_1}{dt} = \frac{d}{dt}\left[C \frac{dV_c}{dt}\right] + \frac{dI_2}{dt} \tag{3.6}$$

By putting (3.6) in (3.2) and after rearranging,

$$V_{in} = L_1 \left[C \frac{d^2 V_c}{dt} + \frac{dI_2}{dt}\right] + V_c \tag{3.7}$$

Substitute the value of V_c from equation (3.5) into the above equation.

$$V_{in} = L_1 \left[C \frac{d^2}{dt}\left(V_u + L_2 \frac{dI_2}{dt}\right) + \frac{dI_2}{dt}\right] + V_u + L_2 \frac{dI_2}{dt} \tag{3.8}$$

Applying Laplace transform and rearranging, we get

$$I_2 = \frac{1}{(L_1 L_2 C)s^3 + (L_1 + L_2)s} V_{in} - \frac{L_1 C s^2 + 1}{(L_1 L_2 C)s^3 + (L_1 + L_2)s} V_u \tag{3.9}$$

Using equation (3.9), the two loops feedback structure can be developed. The output current I_2 can be used as the main feedback control signal The output current is now given by:

$$I_2 = \frac{K}{(L_1 L_2 C)s^3 + (L_1 + L_2)s + K} I_{ref} - \frac{1 + L_1 C s^2}{(L_1 L_2 C)s^3 + (L_1 + L_2)s + K} V_u \tag{3.10}$$

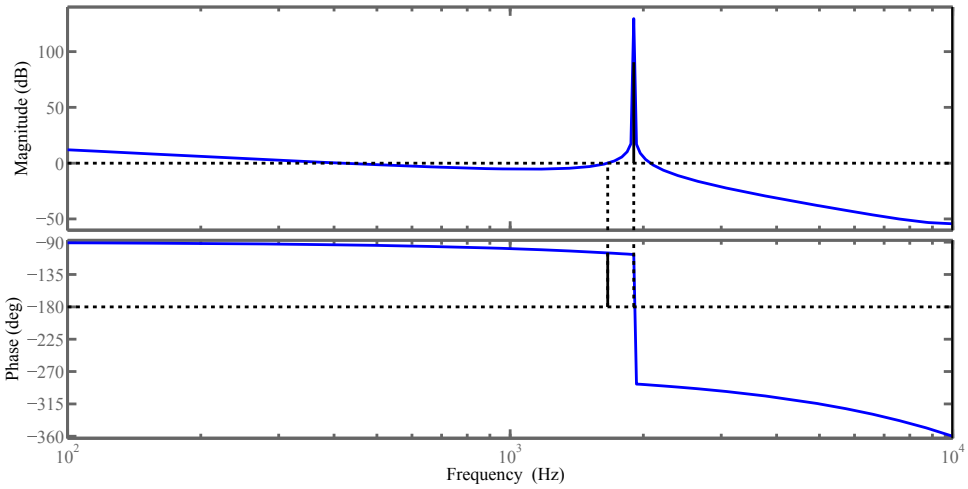

Fig. 3.2: Bode plot of open loop transfer function

3.1.1 Modified transfer function

The open loop bode plot of transfer function is given in 3.2. Bode plots shows that system is not stable by having a negative gain margin of -90.5 dB. So the system is made stable by adding I_c current as feed back which adds the necessary s^2 term in the transfer function as shown in Fig. 3.1. The I_2 is given in the following equation.

$$I_2 = \frac{K}{(L_1L_2C)s^3 + bs^2 + (L_1 + L_2)s + K} I_{ref} - \frac{1 + L_1Cs^2}{(L_1L_2C)s^3 + bs^2 + (L_1 + L_2)s + K} V_u \quad (3.11)$$

However, this method may not be desirable due to the involvement of a double derivative. But it is observed that expression of I_c contains an s^2 term of I_2 such that

$$I_c = L_2Cs^2I_2 + sV_u \quad (3.12)$$

Open loop transfer function $G(s)$ is defined as:

$$G_{ol}(s) = G_p(s) = \frac{I_2}{V_{in}} = \frac{1}{(L_1L_2C)s^3 + K_cL_2Cs^2 + (L_1 + L_2)s} \quad (3.13)$$

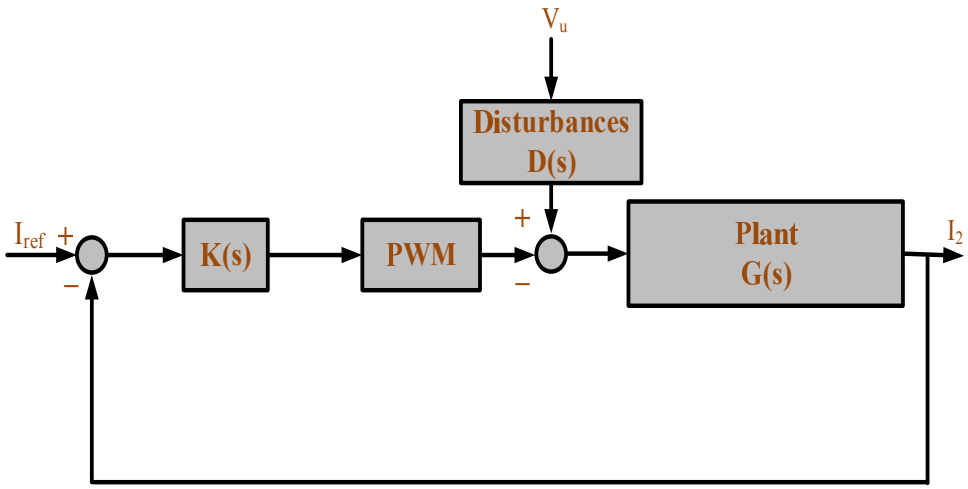

Fig. 3.3: Simplified control system with minor feedback loop of I_c.

And disturbance due to utility is given as $D(s)$:

$$D(s) = L_1 C s^2 + K_c C s + 1 \tag{3.14}$$

Now I_2 becomes:

$$I_2 = \frac{KG(s)}{1 + KG(s)} I_{ref} - \frac{G(s)}{1 + KG(s)} D(s) V_u(s) \tag{3.15}$$

The utility voltage V_u forms a source of disturbance to the system. Ideally, this disturbance can be rejected by implementing a feed-forward loop [56] of exactly the same shape as the utility disturbance transfer function $D(s) = L_1 C s^2 + K_c C s + 1$. Figure 3.4 shows the converter response without using using any controller. Bode plot of converter shows that system is stable by having Gain margin (Gm) 19.1 dB and Phase margin (Pm) 81.2°. However, the plant bandwidth is limited to 5th harmonic which means that converter without any control technique is unable to reject higher order harmonics. So for better quality of output current converter must be designed with a suitable control system.

3.2 Gain Vs Open Loop

The bode plots and root locus of a transfer function aids to make the system stable. They also help to achieve maximum gain without compromising stability.

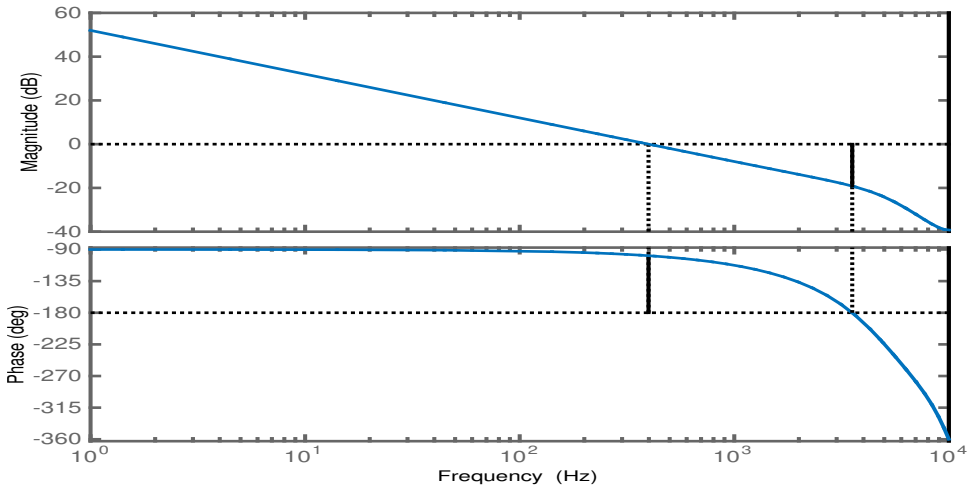

Fig. 3.4: Bode plot of converter response without using any controller

Here in this thesis both the methods are applied to achieve maximum gain so that system remains stable. So the values of L_1, L_2 and C are selected from the table 1.2.

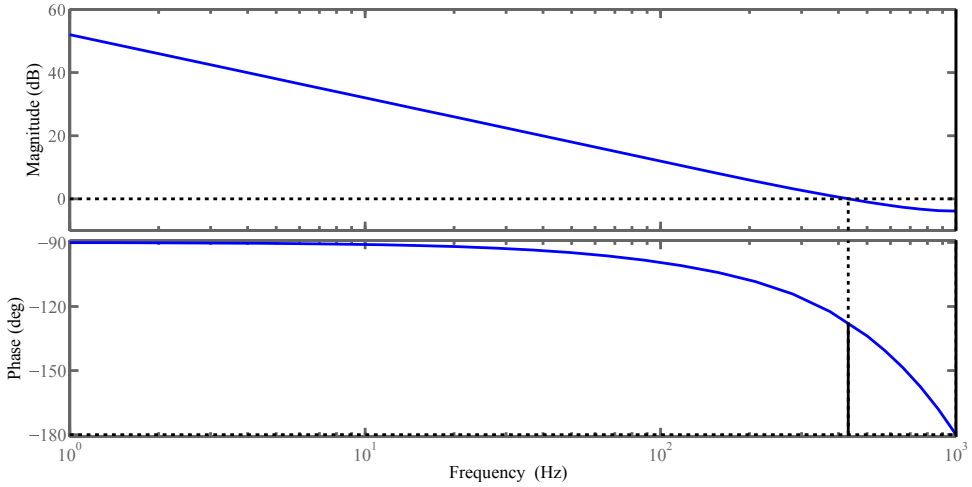

Fig. 3.5: Bode plot of open loop transfer function with Kc=1 gives Gm=3.89 dB and Pm = 52.5 deg.

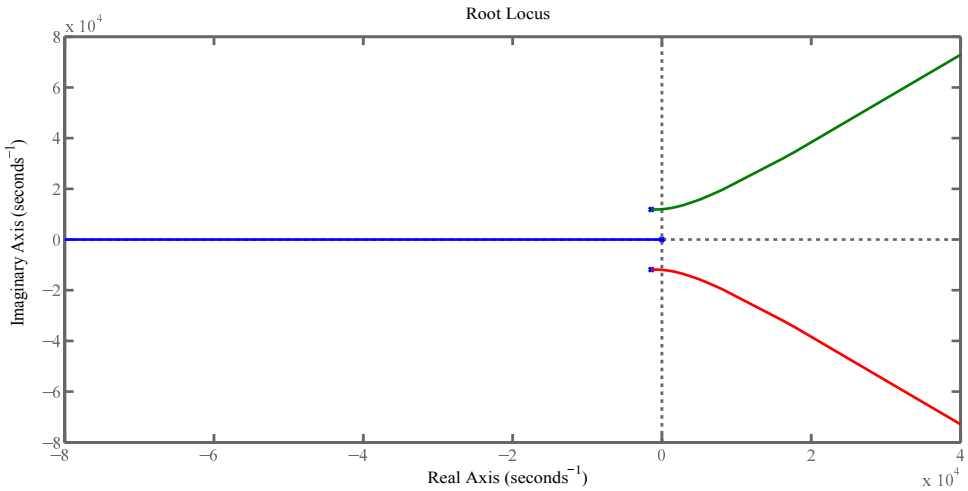

Fig. 3.6: Root Locus of open loop transfer function with Kc=1.

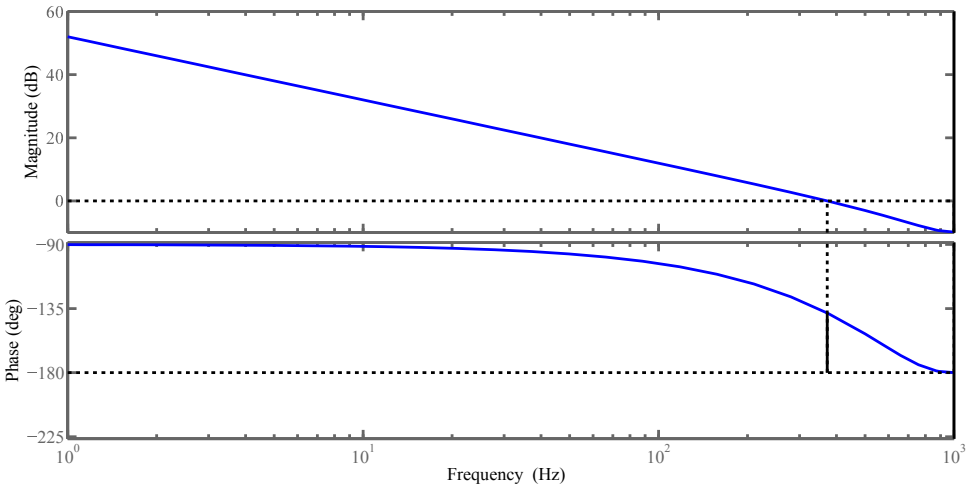

Fig. 3.7: Bode plot of open loop transfer function with Kc=16 gives Gm = 9.88 dB and Pm = 41.9 deg.

We know that system exhibits no oscillatory response when the roots are real. However in this system there are two imaginary roots and one real root as shown in Fig. 3.6, Fig. 3.8, Fig. 3.10. The bode plot of the open loop transfer is showing that the gain margin is very low at K_c=1 and root locus is showing that the poles are close to imaginary axis (Fig. 3.5, Fig. 3.6). So different values of K_c are tried to find a suitable value that can ensure enough gain margin and better system stability. Fig. 3.7 and Fig. 3.8 are plotted by keeping the K_c=16. The gain margin is better and system is well stable by having poles away from the imaginary axis. So by increasing the inner loop gain (K_c) system is moving away from the right half plane which is necessary for stability. Fig. 3.9 and Fig. 3.10

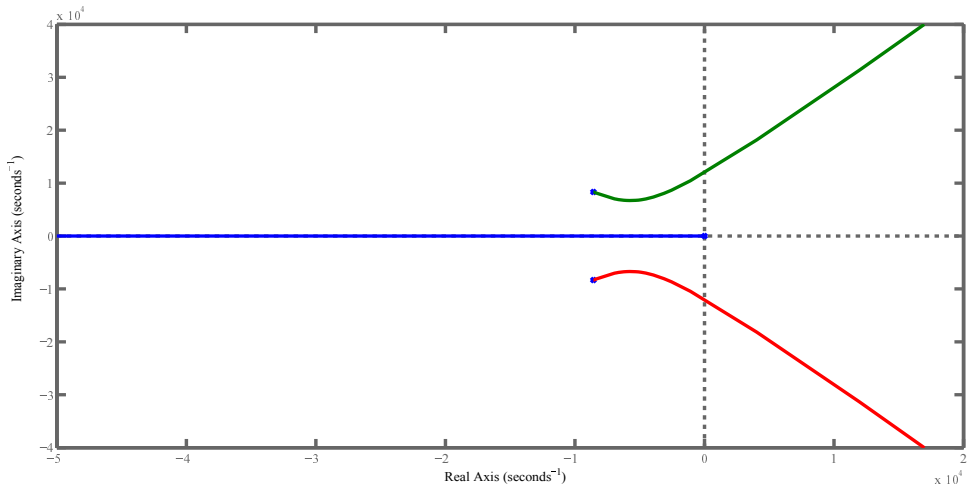

Fig. 3.8: Root Locus of open loop transfer function with Kc=16.

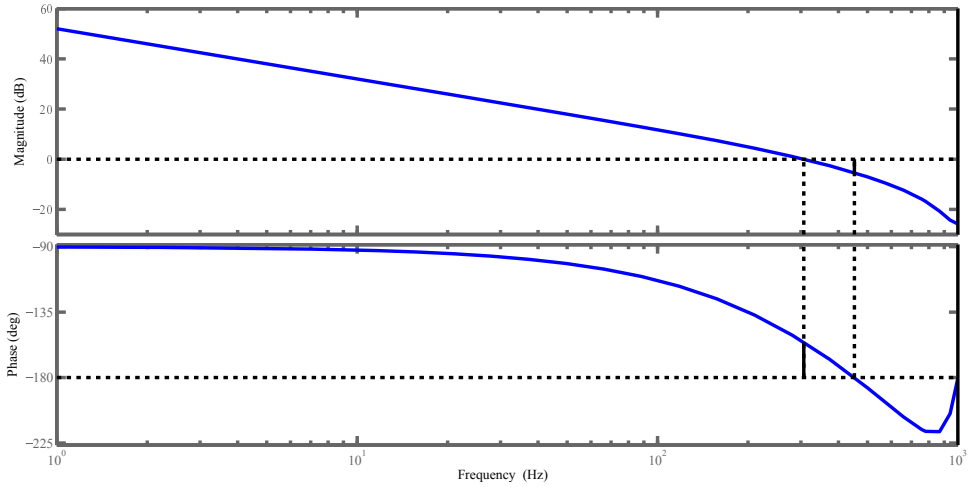

Fig. 3.9: Bode plot of open loop transfer function with Kc=20 Gm = 5.41 dB and Pm = 24.3 deg.

are plotted by setting the value of K_c=20. It is quite obvious that gain margin is decreased and root locus is showing that system poles are again moving towards right half plane which can cause instability. So it was found that the maximum gain that can be achieved without moving poles into the instability region is 16. By choosing the gain value of 16 the gain margin (Gm) is 9.88 dB and phase margin (Pm) is 41.9 degree.

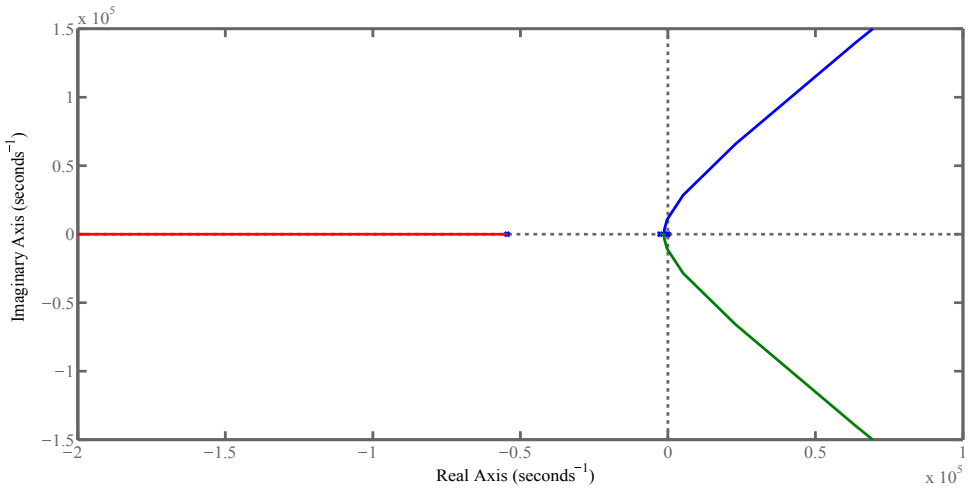

Fig. 3.10: Root Locus of open loop transfer function with Kc=20.

3.3 Designing of Classical Controller

A closed loop feedback system based on a proportional controller was simulated using the system parameters in Table 1.2,. Now capacitance value of the LCL filter is selected C=22.5 μF. The controller gains need to be carefully selected to ensure stability. If the inner loop gain $K_c = 16$ is fixed and outer loop gain is varied such that proportional gain K_p from $1 \rightarrow 3$ and integral gain K_i from $1 \rightarrow 3$, then it is observed that suitable values of proportional gain and integral gain are 1.8 and 3 respectively. Fig. 3.11 shows the Bode diagram of output current transfer function with different gains. When the proportional gain K_p is selected to be 1 and integral gain K_i to be 2, the gain and phase margins are higher. The low gains result in poor disturbance rejection. However, when the proportional gain K_p is increased, the system becomes unstable. and results into distorted output current when utility THD is 5.8%. This does not meet the required standards of the disturbance rejection. This issue is briefly described in the next chapter. Moreover, it is interesting to mention here that almost the same performance can be achieved with a simple proportional (P) controller with only proportional controller gain K_p. Therefore, there is not much difference between P or PI control in this application. The transfer function of plant $G(s)$ is given by equation (3.16).

$$G(s) = \frac{1}{(L_1 L_2 C)s^3 + K_c L_2 C s^2 + (L_1 + L_2)s} \tag{3.16}$$

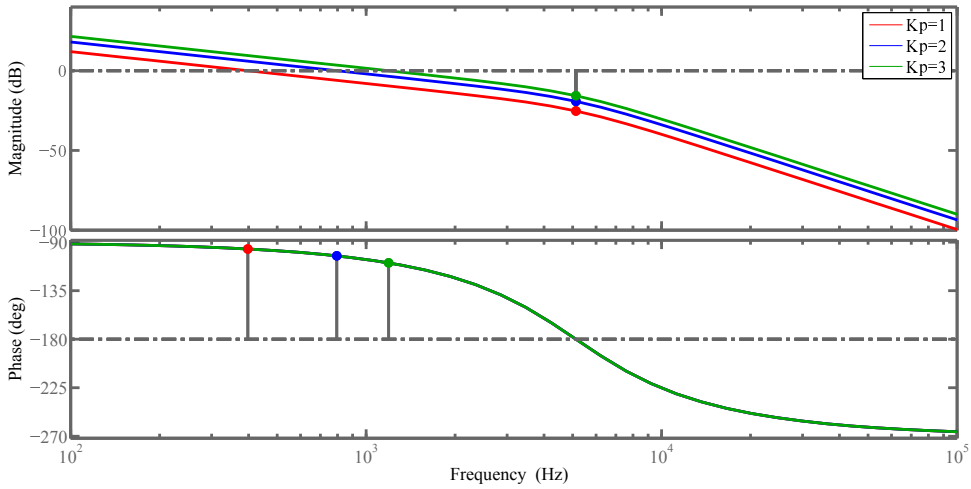

Fig. 3.11: Bode diagram of output current transfer function with classical (PI) controller

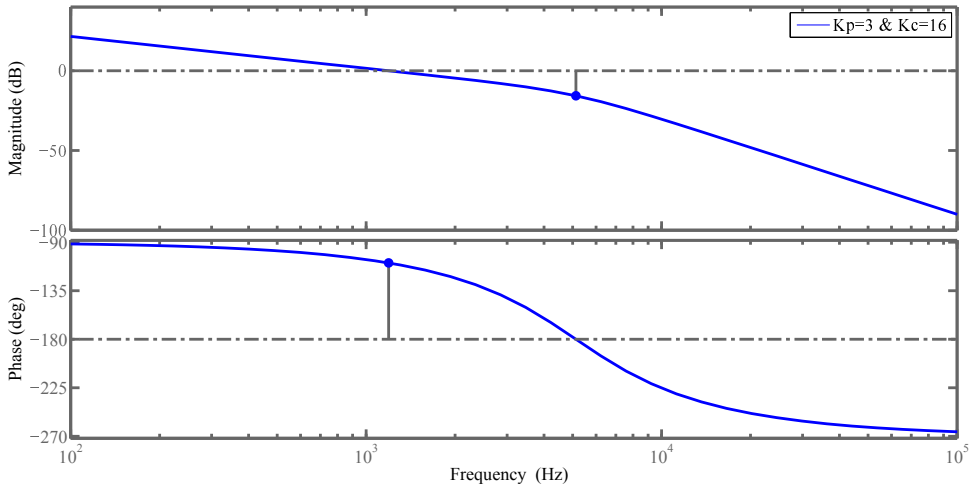

Fig. 3.12: Bode diagram of output current transfer function with K_p=3 and $K_c = 16$

So K_c is selected to be 13 that gives enough damping and K_p to be 3 resulting in GM of 15.7 dB and PM of 70.8° and Bode plot is shown in Fig. 3.12. The loop gain can be easily adjusted to have enough stability as shown in Fig. 3.13. From tuning, it is observed that if the gain is further increased, the system could become either less stable or unstable.

To test the performance of classical controller different levels of harmonics have been added to the utility voltage. Results shows that when the utility THD is more than 5% the classical PI controller is unable to produce an output current as per required standards.

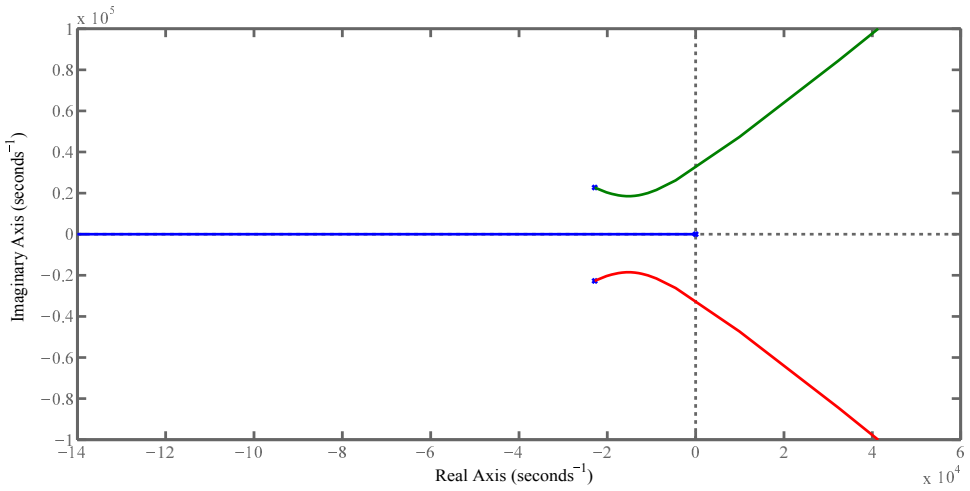

Fig. 3.13: Bode diagram of output current transfer function with K_p=3 and $K_c = 16$

3.4 Proportional Resonant (PR) Controller

The possible solution to avoid complexity, obtain zero steady state error and better disturbance rejection is the use of proportional resonant (PR) controllers, which achieve the same transient and steady state performance as a synchronous (d-q) PI regulators [76, 77]. Proportional resonant (PR) controllers have been widely used for utility connected converters due to their ability to get rid of the steady state error and attenuation of individual harmonics [78–81]. It theoretically introduces an infinite gain at a selected resonance frequency as shown in Fig. 3.14. Fig. 3.15 shows the Bode plot of ideal proportional resonant controller with infinite gains at fundamental frequency, 3rd, 5th and 7th harmonics. Transfer function of ideal PR controller is given in equation (3.17). It can be regarded as an AC regulator/integrator and is similar to an integrator whose infinite DC gain, forces the error to be zero [81]. By having PR control in a stationary frame, there is not much computational effort of transformation involved in synchronous (d-q) regulators and there is the same performance as synchronous (d-q) PI regulators [79].

$$G_{PR0} = K_p + \frac{K_r s}{s^2 + \omega^2} \tag{3.17}$$

The basic PR controller derived by *Zmood and Holmes* [82], can be represented by the transfer function given in equation (3.18). Where, K_p is the proportional

gain, K_r is the gain of resonant term and ω_o is the resonant frequency. This basic PR cannot be implemented in practice due to the demand of infinite gain at resonant frequencies from either an analog or digital system. Normally, it is modified by introducing a new term, quality factor Q , as shown in equation (3.19). Additional selective compensators can be added to equation (3.19) to

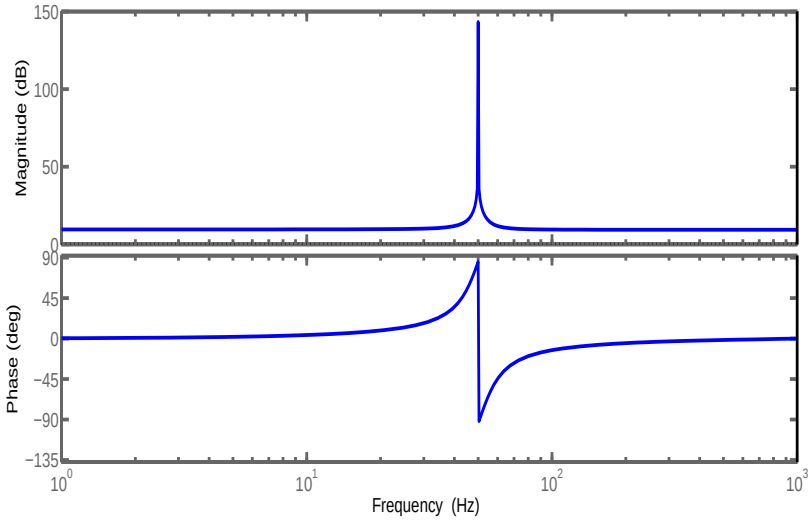

Fig. 3.14: Bode plot of ideal proportional resonant controller

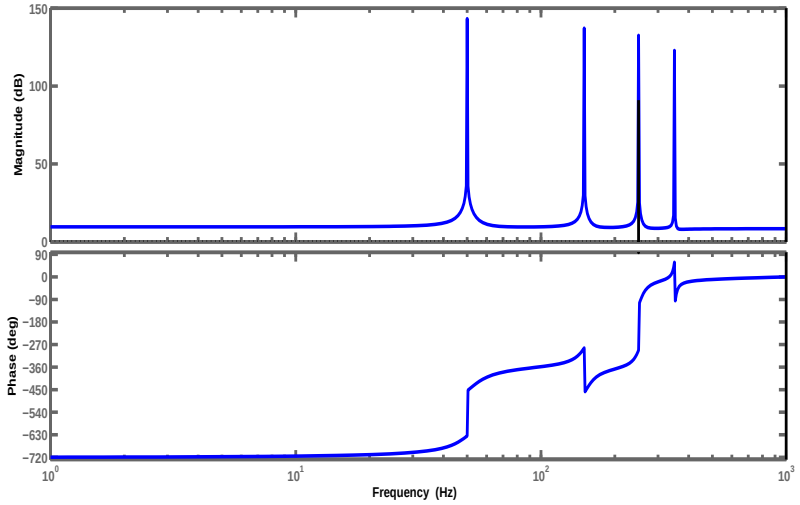

Fig. 3.15: Bode plot of ideal proportional resonant controller with infinite gains at fundamental frequency, 3rd, 5th and 7th harmonics.

reject selective harmonics such as third, fifth and seventh order as represented by equation (3.20).

$$G_{PR1}(s) = K_p + \frac{K_r \omega_o s}{s^2 + \omega_o^2} \tag{3.18}$$

$$G_{PR2}(s) = K_p + \frac{K_r \omega_o s}{s^2 + (\omega_o/Q)s + \omega_o^2} \tag{3.19}$$

$$G_{PR3}(s) = K_p + \frac{K_r \omega_o s}{s^2 + (\omega_o/Q)s + \omega_o^2} + \sum_{h=3,5,7} \frac{K_{rh}(h\omega_o)s}{s^2 + (h\omega_o/Q)s + (h\omega_o)^2} \tag{3.20}$$

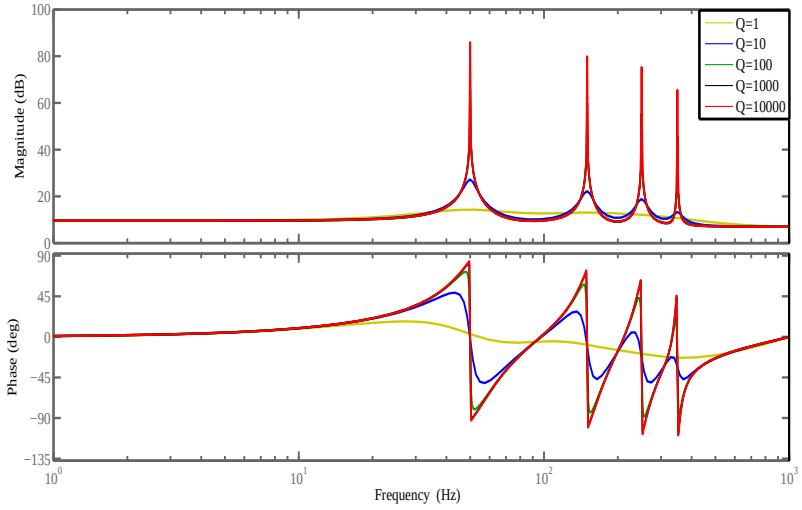

Fig. 3.16: Bode plot of modified proportional resonant controller with infinite gain by varying Q values at fundamental frequency, 3rd, 5th and 7th harmonics.

Fig. 3.16 shows that by increasing the value Q factor, gain is increased but gives a narrow bandpass region at resonant frequency. Whereas, when the value of Q factor is decreased, lower gain value and higher steady state error is produced. So, for better reference tracking and higher disturbance rejection, higher value of Q factor is selected. The value of $K_p = 3$ and $K_r = 2$.

Fig. 3.17 shows the Bode plot of modified proportional resonant controller when the value of K_p changes from 1→1000. It is obvious from the figure that for all the frequencies the gain increases when the value of K_p increases but results in lower bandwidth and decrease in amplitude of the phase. The value of $Q = 1000$ and $K_r = 2$.

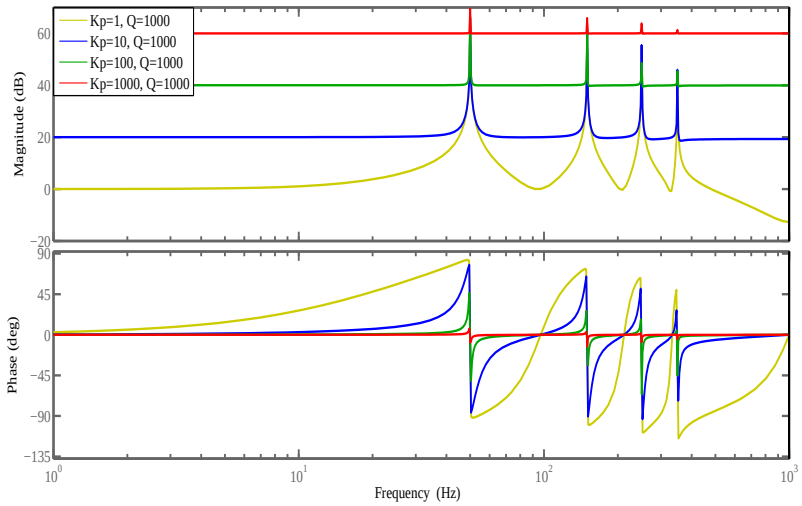

Fig. 3.17: Bode plot of modified proportional resonant controller when K_p value changes.

Chapter 4
Implementation

Performance of classical controller and proportional resonant controller is examined considering different parameters including plant's bandwidth, total harmonic distortion in the output current under varying utility THD, varying capacitance value and varying L_2 value of LCL filter, steady state error etc.

4.1 Analysis of Classical Controller

Classical controller is analysed by considering quality of output current THD, steady state error, plant bandwidth and transient response. To increase utility THD, different levels of harmonics shown in Table 4.1 have been added to the utility voltage to evaluate the performance of the controller. Results from Table 4.2 shows that when the utility THD is more than 5% the classical PI controller is unable to produce an output current as per required standards. This is due to the low gain, higher steady state error and poor disturbance rejection of the PI controller at the utility harmonic frequencies. The results given in Fig. 4.1, Fig. 4.2 are for the values when utility harmonics are 2.7 % and 10.44 %. The derivatives of utility voltage are obtained by offline calculation using a well-known nominal value (230 V rms) of utility voltage. This method has been selected for its simplicity and its ability to produce an output current quality as per required standards. Moreover, it is interesting to mention here that almost the same performance can be achieved with a simple proportional (P) controller with only proportional controller gain K_p. Therefore, there is not much difference between P or PI control in this application.

The research carried out by (*mohsin*) in [24] showed that by having $K_p = 1$ and $K_i = 1$, the suitable transient response can be achieved without oscillations by introducing step change t=0.0455 seconds. However, when $K_p = 2$ and $K_i = 1$, the oscillations were observed [24].

In this study reference current is 100 A. It is obvious from the Fig. 4.1, Fig. 4.2, there exists steady state error. So classical controller fails to follow the reference

Table 4.1: Output Current THD Under Different Utility Voltage Harmonics using RC.

Harmonic number (n)	**Case I** Fundamental Component of Utility Voltage V(rms)	**Case II** Fundamental Component of Utility Voltage V(rms)
3^{rd}	2.4	18.4
5^{th}	4.22	11.5
7^{th}	1.95	9.2
9^{th}	2.37	4.6
11^{th}	1.46	0.115
13^{th}	1.95	0.057
15^{th}	0.455	0.23
17^{th}	065	0.23
19^{th}	0.585	0.23
Utility Voltage THD	2.74%	10.44%

Table 4.2: Percentage THD of output current with PI controller

No.	**Controller Gains** K_p	K_i	**Utility THD** (%)	**Output Current THD** (%)
Case 1	1.8	2	2.7	6.3
	3	1		5.4
	2.3	3		6.5
Case 2	1.8	1	10.44	20.8
	3	1		20.6
	2.3	3		20.4

current when utility THD increases.

The plant bandwidth can be defined as the frequency where Gain margin intersects zero crossing. Fig. 4.3 shows the plant bandwidth with classical controller.

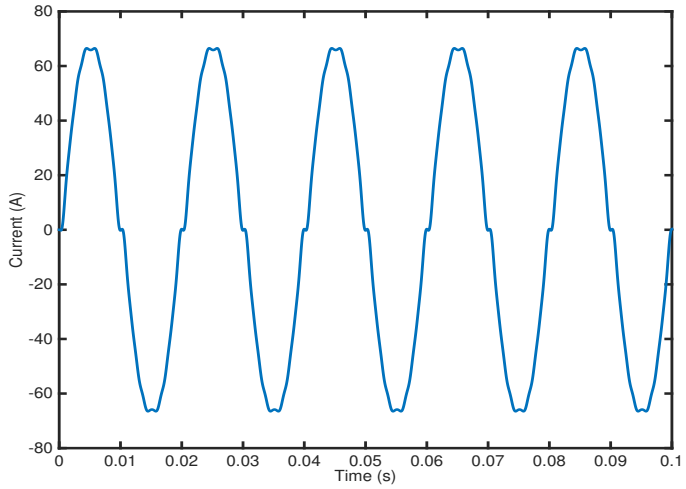

Fig. 4.1: Output current of the two-level converter with PI control when utility harmonics = 2.7 %

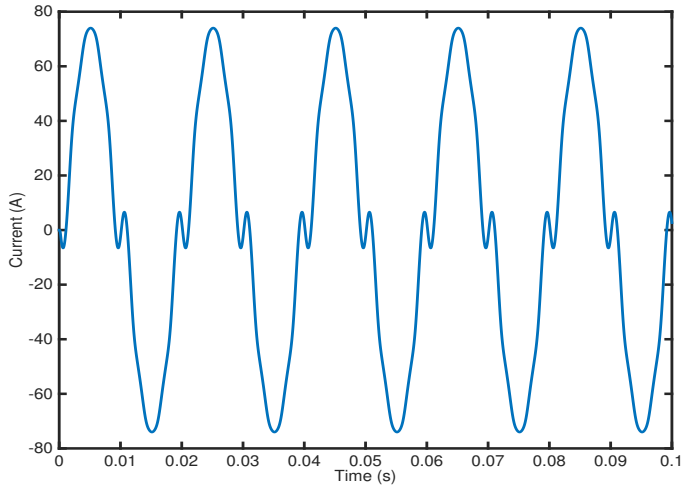

Fig. 4.2: Output current of the two-level converter with PI control when utility harmonics = 10.44 %

It can be seen that the plant has sufficient bandwidth which means that system is able to reject higher order harmonics. However, two level converter using classical control fails to provide better quality of output current due to higher THD, steady state error and also not able to follow the reference current under transient conditions. So there must be used some other control strategy to address all these issue.

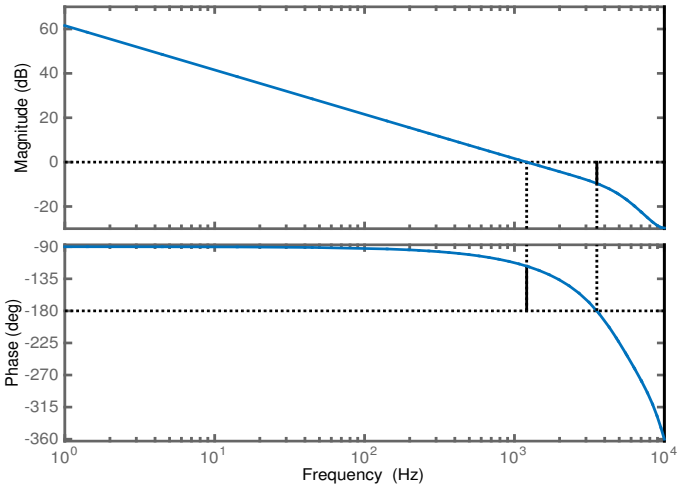

Fig. 4.3: Converter response with classical controller

4.2 Proportional Resonant (PR) Controller

Classical controller fails to provide satisfactory performance as per ANSI/IEEE Standard 519-1992 (IEEE Standard 519, 1993). Classical controller fails due to two well known drawbacks: it is unable to follow a sinusoidal reference without steady state error and also exhibits poor disturbance rejection capability. In order to tackle all these problems, A proportional resonant (PR) controller is used in this study. The PR controller offers an infinite gain at a given frequency and almost no attenuation outside this frequency. Therefore, the PR controller is better choice to eliminate the selective harmonics in a very suitable way.

In order to test the performance of PR controller under varying different utility voltage two cases are used as given in Table 4.1. PR controller is found to be efficient in rejecting undesired harmonics. The Fig. 4.4 is showing the output current quality when utility THD was 2.7 %. The resultant current waveform contains 2.1 % THD which satisfies the ANSI/IEEE Standard 519-1992 (IEEE Standard 519, 1993). There is almost zero steady state error in the output current waveform.

PR controller is also tested under worst case scenario i.e. case 2 of Table 4.2 when utility THD is about 10.44 %. Fig. 4.5 is showing the output current under worst case scenario. The output current waveform contains 3.7 % THD which satisfies the ANSI/IEEE Standard 519-1992 (IEEE Standard 519, 1993). The controller is also ensuring better reference tracking i.e. 100 A by minimizing the

steady state error.

PR controller offers sufficient bandwidth which means converter using PR control is able to reject higher order harmonics. Fig. 4.6 shows the converter response when PR control is used. The gain margin (Gm) is 9.2 % and phase margin (Pm) is 34.4 °.

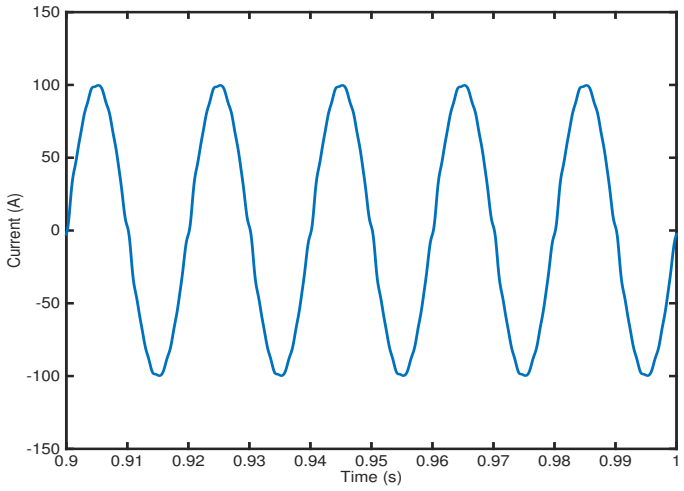

Fig. 4.4: Output current of the two-level converter with PR control when utility harmonics = 2.7 %

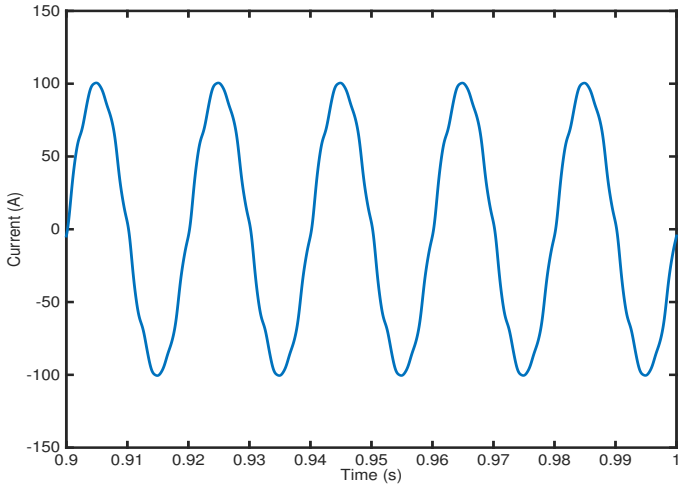

Fig. 4.5: Output current of the two-level converter with PR control when utility harmonics = 10.44 %

4.2.1 Performance of PR controller by varying capacitance of LCL filter

Robustness of two level converter using PR controller is tested under varying the capacitance value of LCL filter. The corresponding Bode plot is shown in the Fig. 4.7. The value of capacitance in LCL filter is changed to ensure that the converter is able to tackle these changes with enough stability margins. It can be seen from the Bode plot that the system can handle the variations in the the capacitance value of filter parameters without being unstable.

4.2.2 Robustness of PR controller by varying L_2 value

Testing the PR controller based system under varying utility impedance L_2 is significant because the grid inductor acts as a coupling point between the grid and the converter. Furthermore, value of utility impedance changes depending on the site where converter is installed. To keep the system stable under worst conditions this uncertainty needs to be investigated. To study the behaviour of the system under varying the L_2 value a Bode plot is given in Fig. 4.8. It can be seen that the system remains stable by having enough gain and phase margins under varying impedance value of grid. So it can be concluded that the system with PR control can tackle variation in utility impedance well enough as shown in Fig. 4.8. Thus, the system is robust against uncertainties in utility impedance

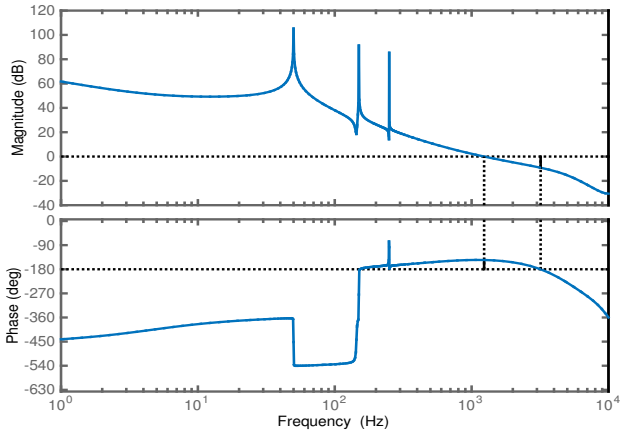

Fig. 4.6: Converter response with PR control

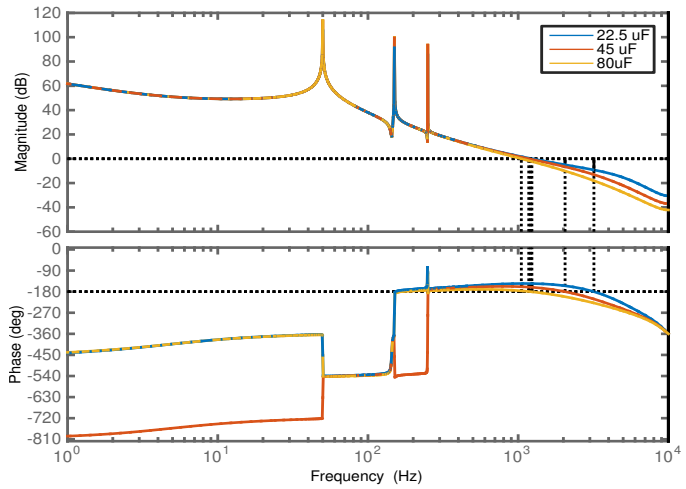

Fig. 4.7: Bode plot of converter response by varying capacitance value of LCL filter

variations. A detailed performance comparison of classical controller and PR controller is given in Table 4.3 and Table 4.4.

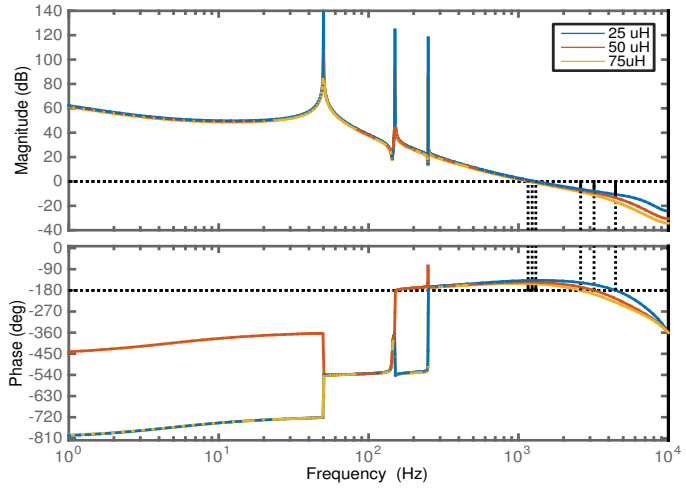

Fig. 4.8: Bode plot of converter response by varying inductance value of LCL filter

Table 4.3: Performance Comparison of PI & PR Controller

Comparison of PI and PR controller based system		
Parameters	PI performance	PR performance
THD (case 1) THD (case 2)	5.4 % 20.6 %	2.1 % 3.7 %
Steady state error	Yes	No
Plant bandwidth	Sufficient	Sufficient
Transient response	Poor	Satisfactory
Control	Easy	Difficult
C variation	Poor	Satisfactory
L_2 Variation	Poor	Satisfactory

Table 4.4: Performance Comparison of Closed Loop System

Comparison of Closed Loop System				
Parameters	Gain Margin	Phase Margin	Close Loop	Output current quality
Without controller	19.1 dB	81.2 deg	Stable	Poor
PI performance	9.61 dB	62.5 deg	Stable	Poor
PR performance	9.62 dB	34.6 deg	Stable	Better

Chapter 5
Conclusion and Recommendation

This chapter summarises and analyses the research related to the application of a classical and PR controller for a two-level LCL filter based converter, carried out in this thesis. Particular attention has been focused on the contributions made in the field by comparing different methods and approaches. The issues and limitations raised during the research have been addressed by making suggestions for future work.

5.1 Summary of the thesis

The overall aim of this research has been to investigate the limitation of classical control and performance of PR control for utility connected two-level LCL filter based converters. The work presented in this thesis consists of two parts, first, an evaluation of the performance of classical control (PI) for LCL filter based two-level converters (chapter 2), and second, the analysis of PR for the two level converter (chapter 3).

Chapter 1 discussed the significance of the power electronic converters within microgrids, which can address the limitations of current power systems by promoting distributed generators including renewable energy sources. Among different available topologies of these converters, two-level LCL filter based topology has been adopted by describing its features for the purpose of current control in the utility connected mode. This chapter described the main contributions and presented a general outline of the thesis.

Chapter 2 selected the suitable structure of the two-level utility connected converter by looking at the methods of dampening the resonance due to the LCL filters. The problems attached with different controllers were critically reviewed. Different parameters are described for evaluating the the suitable current control for two level grid connected inverter in this thesis. The transfer function of PR is given in chapter 3.

Chapter 3 describes the brief modelling of two level converter. Different structures are explained and finally a simplified structure is adopted for analysis. Designing of classical control is briefly given in this chapter. PR control and its working principal is given at the end of this chapter.

The performance of classical controller and PR controller is tested under varying utility THD in chapter 4. Fundamental investigations were carried out into stability constraints, a trade-off between steady state error and system transient response for the design of the PI and PR control. It was concluded that PR controller can provided fast error convergence as compared to PI control. The output current had low THD without almost zero steady state error when PR control was used.

5.2 Conclusion

Two level converter with LCL filter was made stable by using conventional PI controller. A stable conventional (PI) two loops feedback system was designed for the two-level current control of grid connected inverter. Results obtained by changing different parameters are presented. It is found that classical control is not able to provide better quality of current. Classical control has steady state state error and unable to suppress harmonics. PR control is adopted to address the limitations of PI control. Results indicate that appropriate bandwidth can be obtained if parameters are selected wisely. Quality of output current is better than Pi control. There is almost zero steady state error. Simulation results are given which confirm that by using PR controller, quality of output current improves in terms of THD and steady state error. The output current meet the international standards even under the influence of utility THD exceeds 5%.

References

[1] J. Lopes, "Advanced microgrids as a component for active management of distribution networks," in *Power Engineering, Energy and Electrical Drives, 2009. POWERENG '09. International Conference on*, March 2009, pp. 7–8. 1

[2] F. Nejabatkhah and Y. W. Li, "Overview of power management strategies of hybrid ac x002f;dc microgrid," *Power Electronics, IEEE Transactions on*, vol. 30, no. 12, pp. 7072–7089, Dec 2015. 1

[3] R. Anderson, A. Boulanger, W. Powell, and W. Scott, "Adaptive stochastic control for the smart grid," *Proceedings of the IEEE*, vol. 99, no. 6, pp. 1098–1115, June 2011. 1

[4] D. Wang and F. Z. Peng, "Smart gateway grid: A dg-based residential electric power supply system," *Smart Grid, IEEE Transactions on*, vol. 3, no. 4, pp. 2232–2239, Dec 2012. 1

[5] S. Chowdhury, S. Chowdhury, C. Ten, and P. Crossley, "Operation and control of dg based power island in smart grid environment," in *Electricity Distribution - Part 1, 2009. CIRED 2009. 20th International Conference and Exhibition on*, June 2009, pp. 1–5. 1

[6] F. Blaabjerg, Z. Chen, and S. Kjaer, "Power electronics as efficient interface in dispersed power generation systems," *Power Electronics, IEEE Transactions on*, vol. 19, no. 5, pp. 1184–1194, Sept 2004. 1

[7] S. Kjaer, J. Pedersen, and F. Blaabjerg, "A review of single-phase grid-connected inverters for photovoltaic modules," *Industry Applications, IEEE Transactions on*, vol. 41, no. 5, pp. 1292–1306, Sept 2005. 1

[8] "Bp statistical review of world energy," Energy Academy, Heriot-Watt University, 2014, accessed: 2015-06-10. 1

[9] B. Bose, "Global warming: Energy, environmental pollution, and the impact of power electronics," *Industrial Electronics Magazine, IEEE*, vol. 4, no. 1, pp. 6–17, March 2010. 1

[10] L. Barroso, H. Rudnick, F. Sensfuss, and P. Linares, "The green effect," *Power and Energy Magazine, IEEE*, vol. 8, no. 5, pp. 22–35, Sept 2010. 1

[11] J. Guerrero, F. Blaabjerg, T. Zhelev, K. Hemmes, E. Monmasson, S. Jemei, M. Comech, R. Granadino, and J. Frau, "Distributed generation: Toward a new energy paradigm," *Industrial Electronics Magazine, IEEE*, vol. 4, no. 1, pp. 52–64, March 2010. 1

[12] M. Jamil, B. Hussain, M. Abu-Sara, R. Boltryk, and S. Sharkh, "Microgrid power electronic converters: State of the art and future challenges," in *Universities Power Engineering Conference (UPEC), 2009 Proceedings of the 44th International*, Sept 2009, pp. 1–5. 1

[13] N. Yektay, A. Darudi, and M. Javidi, "An optimal power flow control method for grid-connected inverters," in *Environment and Electrical Engineering (EEEIC), 2013 13th International Conference on*, Nov 2013, pp. 260–265. 1

[14] T. Basso and R. DeBlasio, "Ieee 1547 series of standards: interconnection issues," *Power Electronics, IEEE Transactions on*, vol. 19, no. 5, pp. 1159–1162, Sept 2004. 2

[15] "Ieee recommended practice for utility interface of photovoltaic (pv) systems," *IEEE Std 929-2000*, pp. i–, 2000. 2

[16] "Ieee recommended practices and requirements for harmonic control in electrical power systems," *IEEE Std 519-1992*, pp. 1–112, April 1993. 2

[17] F. Blaabjerg, R. Teodorescu, M. Liserre, and A. Timbus, "Overview of control and grid synchronization for distributed power generation systems," *Industrial Electronics, IEEE Transactions on*, vol. 53, no. 5, pp. 1398–1409, Oct 2006. 3

[18] S. Dasgupta, S. Sahoo, and S. Panda, "Single-phase inverter control techniques for interfacing renewable energy sources with microgrid #x2014;part i: Parallel-connected inverter topology with active and reactive power flow control along with grid current shaping," *Power Electronics, IEEE Transactions on*, vol. 26, no. 3, pp. 717–731, March 2011. 3

[19] S. Kouro, M. Malinowski, K. Gopakumar, J. Pou, L. Franquelo, B. Wu, J. Rodriguez, M. Perez, and J. Leon, "Recent advances and industrial applications of multilevel converters," *Industrial Electronics, IEEE Transactions on*, vol. 57, no. 8, pp. 2553–2580, Aug 2010. 3

[20] J. Barros, J. Silva, and E. Jesus, "Fast-predictive optimal control of npc multilevel converters," *Industrial Electronics, IEEE Transactions on*, vol. 60, no. 2, pp. 619–627, Feb 2013. 3

[21] E. Babaei, M. Kangarlu, and M. Sabahi, "Extended multilevel converters: an attempt to reduce the number of independent dc voltage sources in cascaded multilevel converters," *Power Electronics, IET*, vol. 7, no. 1, pp. 157–166, January 2014. 3

[22] I. Sefa and O. Ozdemir, "Experimental study of interleaved mppt converter for pv systems," in *Industrial Electronics, 2009. IECON '09. 35th Annual Conference of IEEE*, Nov 2009, pp. 456–461. 3

[23] F. Bouchafaa, D. Beriber, and M. Boucherit, "Modeling and control of a gird connected pv generation system," in *Control Automation (MED), 2010 18th Mediterranean Conference on*, June 2010, pp. 315–320. 3

[24] M. Jamil, "Repetitive current control of two-level and interleaved three-phase pwm utility connected converters," Ph.D. dissertation, Faculty of Engineering and the EnvironmentEngineering Sciences, University of Southampton, 2012. 3, 22, 41

[25] A. Timbus, M. Ciobotaru, R. Teodorescu, and F. Blaabjerg, "Adaptive resonant controller for grid-connected converters in distributed power generation systems," in *Applied Power Electronics Conference and Exposition, 2006. APEC '06. Twenty-First Annual IEEE*, March 2006, pp. 6 pp.–. 5

[26] Y.-R. Mohamed and E. El-Saadany, "An improved deadbeat current control scheme with a novel adaptive self-tuning load model for a three-phase pwm voltage-source inverter," *Industrial Electronics, IEEE Transactions on*, vol. 54, no. 2, pp. 747–759, April 2007. 5

[27] J. Espi, J. Castello, R. Garcia-Gil, G. Garcera, and E. Figueres, "An adaptive robust predictive current control for three-phase grid-connected inverters,"

Industrial Electronics, IEEE Transactions on, vol. 58, no. 8, pp. 3537–3546, Aug 2011. 5

[28] X. Hao, X. Yang, R. Xie, L. Huang, T. Liu, and Y. Li, "A fixed switching frequency integral resonant sliding mode controller for three-phase grid-connected photovoltaic inverter with lcl-filter," in *ECCE Asia Downunder (ECCE Asia), 2013 IEEE*, June 2013, pp. 793–798. 5

[29] X. Shi, Y. Shen, Z. Wang, J. Zhang, Z. Qian, and F. Peng, "A repetitive-based controller for a hybrid filter with high quality grid current waveform," in *Applied Power Electronics Conference and Exposition (APEC), 2011 Twenty-Sixth Annual IEEE*, March 2011, pp. 757–762. 5

[30] K. Jaesuk and S. Seung-Ki, "Harmonic currents control of three-phase four-wire grid-connected pwm inverter based on high-order repetitive controller," in *Power Electronics and ECCE Asia (ICPE-ECCE Asia), 2015 9th International Conference on*, June 2015, pp. 2161–2166. 5

[31] T.-Y. Doh and J. R. Ryoo, "Add-on type repetitive controller design for the feedback control system satisfying the robust performance condition," in *Asian Control Conference, 2009. ASCC 2009. 7th*, Aug 2009, pp. 1582–1587. 5

[32] X. Shi, Y. Shen, Z. Wang, J. Zhang, Z. Qian, and F. Peng, "A repetitive-based controller for a hybrid filter with high quality grid current waveform," in *Applied Power Electronics Conference and Exposition (APEC), 2011 Twenty-Sixth Annual IEEE*, March 2011, pp. 757–762. 5

[33] A. Khairy, M. Ibrahim, N. Abdel-Rahim, and H. Elsherif, "Comparing proportional-resonant and fuzzy-logic controllers for current controlled single-phase grid-connected pwm dc/ac inverters," in *Renewable Power Generation (RPG 2011), IET Conference on*, Sept 2011, pp. 1–6. 5

[34] H. Hu, W. Wei, Y. Peng, and J. Lei, "Optimized design of damped proportional-resonant controllers for grid-connected inverters through genetic algorithm," in *Electronics and Application Conference and Exposition (PEAC), 2014 International*, Nov 2014, pp. 1265–1270. 5

[35] H. Dehghani Tafti, A. Maswood, A. Ukil, O. Gabriel, and L. Ziyou, "Npc photovoltaic grid-connected inverter using proportional-resonant controller," in *Power and Energy Engineering Conference (APPEEC), 2014 IEEE PES Asia-Pacific*, Dec 2014, pp. 1–6. 5

[36] Y. Li and M. Wang, "Control stratories for grid-connected and island dualmode operated inverter under unbalanced grid voltage conditions," in *Power Electronics and Motion Control Conference (IPEMC), 2012 7th International*, vol. 3, June 2012, pp. 2152–2156. 5

[37] E. Twining and D. Holmes, "Grid current regulation of a three-phase voltage source inverter with an lcl input filter," *Power Electronics, IEEE Transactions on*, vol. 18, no. 3, pp. 888–895, May 2002. 10, 14

[38] W. Wu, Y. He, T. Tang, and F. Blaabjerg, "A new design method for the passive damped lcl and llcl filter-based single-phase grid-tied inverter," *Industrial Electronics, IEEE Transactions on*, vol. 60, no. 10, pp. 4339–4350, Oct 2013. 11

[39] C. Yu, X. Zhang, F. Liu, H. Xu, C. Qiao, Z. Shao, W. Zhao, and H. Ni, "A general active damping method based on capacitor voltage detection for grid-connected inverter," in *ECCE Asia Downunder (ECCE Asia), 2013 IEEE*, June 2013, pp. 829–835. 11

[40] C. Bao, X. Ruan, X. Wang, W. Li, D. Pan, and K. Weng, "Step-by-step controller design for lcl-type grid-connected inverter with capacitor #x2013;current-feedback active-damping," *Power Electronics, IEEE Transactions on*, vol. 29, no. 3, pp. 1239–1253, March 2014. 11

[41] R. Pena-Alzola, M. Liserre, F. Blaabjerg, and Y. Yang, "Robust design of lcl-filters for active damping in grid converters," in *Industrial Electronics Society, IECON 2013 - 39th Annual Conference of the IEEE*, Nov 2013, pp. 1248–1253. 11

[42] G. Zeng and T. Rasmussen, "Design of current-controller with pr-regulator for lcl-filter based grid-connected converter," in *Power Electronics for Distributed Generation Systems (PEDG), 2010 2nd IEEE International Symposium on*, June 2010, pp. 490–494. 11

[43] G. Shen, X. Zhu, J. Zhang, and D. Xu, "A new feedback method for pr current control of lcl-filter-based grid-connected inverter," *Industrial Electronics, IEEE Transactions on*, vol. 57, no. 6, pp. 2033–2041, June 2010. 11

[44] R. Teodorescu, F. Blaabjerg, M. Liserre, and P. Loh, "Proportional-resonant controllers and filters for grid-connected voltage-source converters," *Electric Power Applications, IEE Proceedings*, vol. 153, no. 5, pp. 750–762, September 2006. xi, 11, 12

[45] R. Turner, S. Walton, and R. Duke, "Robust high-performance inverter control using discrete direct-design pole placement," *Industrial Electronics, IEEE Transactions on*, vol. 58, no. 1, pp. 348–357, Jan 2011. 11

[46] B. Li, W. Yao, L. Hang, and L. Tolbert, "Robust proportional resonant regulator for grid-connected voltage source inverter (vsi) using direct pole placement design method," *Power Electronics, IET*, vol. 5, no. 8, pp. 1367–1373, September 2012. 11

[47] M. Liserre, F. Blaabjerg, and S. Hansen, "Design and control of an lcl-filter-based three-phase active rectifier," *Industry Applications, IEEE Transactions on*, vol. 41, no. 5, pp. 1281–1291, Sept 2005. 12

[48] B. Li, W. Yao, L. Hang, and L. Tolbert, "Robust proportional resonant regulator for grid-connected voltage source inverter (vsi) using direct pole placement design method," *Power Electronics, IET*, vol. 5, no. 8, pp. 1367–1373, September 2012. 12

[49] X. Wang, X. Ruan, S. Liu, and C. Tse, "Full feedforward of grid voltage for grid-connected inverter with lcl filter to suppress current distortion due to grid voltage harmonics," *Power Electronics, IEEE Transactions on*, vol. 25, no. 12, pp. 3119–3127, Dec 2010. 12

[50] D. Holmes, T. Lipo, B. McGrath, and W. Kong, "Optimized design of stationary frame three phase ac current regulators," *Power Electronics, IEEE Transactions on*, vol. 24, no. 11, pp. 2417–2426, Nov 2009. 13

[51] Q. Zeng and L. Chang, "An advanced svpwm-based predictive current controller for three-phase inverters in distributed generation systems," *Industrial*

Electronics, IEEE Transactions on, vol. 55, no. 3, pp. 1235–1246, March 2008. 13

[52] W. Li, X. Ruan, D. Pan, and X. Wang, "Full-feedforward schemes of grid voltages for a three-phase lcl -type grid-connected inverter," *Industrial Electronics, IEEE Transactions on*, vol. 60, no. 6, pp. 2237–2250, June 2013. 13

[53] E. Twining and D. Holmes, "Grid current regulation of a three-phase voltage source inverter with an lcl input filter," *Power Electronics, IEEE Transactions on*, vol. 18, no. 3, pp. 888–895, May 2003. 13

[54] Z. F. Hussein, "Current control of three-phase pwm inverter for flywheel energy storage system," Ph.D. dissertation, University of Southampton U.K., 2000. xi, 13, 14, 21

[55] G. Escobar, J. Leyva-Ramos, P. Martinez, and A. Valdez, "A repetitive-based controller for the boost converter to compensate the harmonic distortion of the output voltage," *Control Systems Technology, IEEE Transactions on*, vol. 13, no. 3, pp. 500–508, May 2005. 13

[56] S. M. Abu Sharkh and M. A. Abu-Sara, "Current control of utility-connected two-level and three-level pwm inverters," *European Power Electronics and Drives Journal*, vol. 14, no. 3, pp. 13–18, 2004. xi, 14, 15, 28, 31

[57] A.-S. M. Abu-Sharkh, S.M. and Z. Hussien, "Current control of utility-connected dc-ac three-phase voltage-source inverters using repetitive feedback," in *9th European Conference on Power Electronics and Applications (EPE 01)*, August 2001, pp. 27–29. 14

[58] G. Shen, D. Xu, L. Cao, and X. Zhu, "An improved control strategy for grid-connected voltage source inverters with an lcl filter," *Power Electronics, IEEE Transactions on*, vol. 23, no. 4, pp. 1899–1906, July 2008. xi, 15, 16, 21

[59] C. Cecati, A. Dell'Aquila, and M. Liserre, "A novel three-phase single-stage distributed power inverter," *Power Electronics, IEEE Transactions on*, vol. 19, no. 5, pp. 1226–1233, Sept 2004. 16

[60] X. Zhang, C. Yu, F. Liu, F. Li, and R. Cao, "Stability improvement of grid-connect inverter using combination of passive and active damping," in *Power Electronics and Motion Control Conference (IPEMC), 2012 7th International*, vol. 4, June 2012, pp. 2809–2813. 16

[61] K. Jalili and S. Bernet, "Design of lcl filters of active-front-end two-level voltage-source converters," *Industrial Electronics, IEEE Transactions on*, vol. 56, no. 5, pp. 1674–1689, May 2009. 16

[62] P. Channegowda and V. John, "Filter optimization for grid interactive voltage source inverters," *Industrial Electronics, IEEE Transactions on*, vol. 57, no. 12, pp. 4106–4114, Dec 2010. 16, 19, 20, 21

[63] M. Routimo and H. Tuusa, "Lcl type supply filter for active power filter - comparison of an active and a passive method for resonance damping," in *Power Electronics Specialists Conference, 2007. PESC 2007. IEEE*, June 2007, pp. 2939–2945. 17

[64] H. Cha and T.-K. Vu, "Comparative analysis of low-pass output filter for single-phase grid-connected photovoltaic inverter," in *Applied Power Electronics Conference and Exposition (APEC), 2010 Twenty-Fifth Annual IEEE*, Feb 2010, pp. 1659–1665. 19

[65] A.-S. Luiz and B. Filho, "Analysis of passive filters for high power three-level rectifiers," in *Industrial Electronics, 2008. IECON 2008. 34th Annual Conference of IEEE*, Nov 2008, pp. 3207–3212. 19

[66] A. Balasubramanian and V. John, "Analysis and design of split-capacitor resistiveinductive passive damping for lcl filters in grid-connected inverters," *Power Electronics, IET*, vol. 6, no. 9, pp. 1822–1832, November 2013. 19, 20

[67] A. Rockhill, M. Liserre, R. Teodorescu, and P. Rodriguez, "Grid-filter design for a multimegawatt medium-voltage voltage-source inverter," *Industrial Electronics, IEEE Transactions on*, vol. 58, no. 4, pp. 1205–1217, April 2011. 20

[68] G. Zeng, T. Rasmussen, L. Ma, and R. Teodorescu, "Design and control of lcl-filter with active damping for active power filter," in *Industrial Electronics (ISIE), 2010 IEEE International Symposium on*, July 2010, pp. 2557–2562. 20

[69] D. Wojciechowski and R. Strzelecki, "Predictive control of active filter system with lcl coupling circuit," in *Power Electronics Conference (IPEC), 2010 International*, June 2010, pp. 2276–2282. 20

[70] J. Dannehl, M. Liserre, and F. Fuchs, "Filter-based active damping of voltage source converters with lcl filter," *Industrial Electronics, IEEE Transactions on*, vol. 58, no. 8, pp. 3623–3633, Aug 2011. 20

[71] G. Shen, X. Zhu, J. Zhang, and D. Xu, "A new feedback method for pr current control of lcl-filter-based grid-connected inverter," *Industrial Electronics, IEEE Transactions on*, vol. 57, no. 6, pp. 2033–2041, June 2010. xi, 21, 22

[72] W. Zhao and G. Chen, "Comparison of active and passive damping methods for application in high power active power filter with lcl-filter," in *Sustainable Power Generation and Supply, 2009. SUPERGEN '09. International Conference on*, April 2009, pp. 1–6. 21

[73] M. A. Abusara, "Digital control of utility and parallel connected three-phase pwm inverters," Ph.D. dissertation, University of Southampton U.K., 2004. 21

[74] N. Mukherjee and D. De, "Analysis and improvement of performance in lcl filter-based pwm rectifier/inverter application using hybrid damping approach," *Power Electronics, IET*, vol. 6, no. 2, pp. 309–325, Feb 2013. 22, 23

[75] Y. Tang, P. C. Loh, P. Wang, F. H. Choo, F. Gao, and F. Blaabjerg, "Generalized design of high performance shunt active power filter with output lcl filter," *Industrial Electronics, IEEE Transactions on*, vol. 59, no. 3, pp. 1443–1452, March 2012. 27

[76] G. Shen, X. Zhu, J. Zhang, and D. Xu, "A new feedback method for pr current control of lcl-filter-based grid-connected inverter," *Industrial Electronics, IEEE Transactions on*, vol. 57, no. 6, pp. 2033–2041, June 2010. 37

[77] S.-Y. Park, C.-L. Chen, J.-S. Lai, and S.-R. Moon, "Admittance compensation in current loop control for a grid-tie lcl fuel cell inverter," *Power*

Electronics, IEEE Transactions on, vol. 23, no. 4, pp. 1716–1723, July 2008. 37

[78] F. Liu and X. Zha, "Research on control strategy combining pole-assignment and pr control in three-phase grid-connected inverter," in *Power Electronics and Motion Control Conference, 2009. IPEMC '09. IEEE 6th International*, May 2009, pp. 2170–2173. 37

[79] Y. Yang, K. Zhou, and F. Blaabjerg, "Enhancing the frequency adaptability of periodic current controllers for grid-connected power converters," in *Energy Conversion Congress and Exposition (ECCE), 2015 IEEE*, Sept 2015, pp. 5998–6005. 37

[80] G. Shen, X. Zhu, J. Zhang, and D. Xu, "A new feedback method for pr current control of lcl-filter-based grid-connected inverter," *Industrial Electronics, IEEE Transactions on*, vol. 57, no. 6, pp. 2033–2041, June 2010. 37

[81] S. Zhou and J. Liu, "Analysis and comparison of resonant-based current controllers implemented in stationary reference frame: A complex pole-zero placement perspective," in *Energy Conversion Congress and Exposition (ECCE), 2015 IEEE*, Sept 2015, pp. 1624–1631. 37

[82] D. Zmood, D. Holmes, and G. Bode, "Frequency-domain analysis of three-phase linear current regulators," *Industry Applications, IEEE Transactions on*, vol. 37, no. 2, pp. 601–610, Mar 2001. 37

APPENDIX-PUBLICATIONS